Rapid Acquisition of Alectinib Resistance in *ALK*-positive Lung Cancer with High Tumor Mutation Burden

Go Makimoto[a], Kadoaki Ohashi[a,b]*, Shuta Tomida[c], Kazuya Nishii[a], Takehiro Matsubara[c], Hiroe Kayatani[a], Hisao Higo[a], Kiichiro Ninomiya[a], Akiko Sato[b], Hiromi Watanabe[a], Hirohisa Kano[a], Takashi Ninomiya[b], Toshio Kubo[d], Kammei Rai[b], Eiki Ichihara[b], Katsuyuki Hotta[e], Masahiro Tabata[d], Shinichi Toyooka[c,f], Minoru Takata[g], Yoshinobu Maeda[a], and Katsuyuki Kiura[b]

[a] Department of Hematology, Oncology and Respiratory Medicine, Okayama University Graduate School of Medicine, Dentistry and Pharmaceutical Sciences,

[b] Department of Respiratory Medicine, Okayama University Hospital,

[c] Okayama University Hospital Biobank, Okayama University Hospital,

[d] Center for Clinical Oncology, Okayama University Hospital,

[e] Center of Innovative Clinical Medicine, Okayama University Hospital,

[f] Department of Thoracic surgery, Okayama University Hospital

2-5-1 Shikata-cho Kita Ward, Okayama 700-8558, Japan

[g] Laboratory of DNA Damage Signaling, Department of Late Effects Studies, Graduate School of Biostudies, Radiation Biology Center, Kyoto University, Yoshidakonoe-cho, Sakyo-ku, Kyoto 606-8501, Japan

Financial support

This research received a specific grant from JSPS Grant-in-Aid for Scientific Research [Grant-in-Aid for Young Scientists (B): KAKEN 16K19454 to K.O.] and JSPS Grants-in-Aid for Scientific Research [Scientific Research (B): KAKEN 15H04830 to K.O., T.K., and K.K.]. This research was also supported by a Grant for Lung Cancer Research (K.O.) provided by the

Japan Lung Cancer Society.

*** Corresponding author.**

Department of Respiratory Medicine, Okayama University Hospital, 2-5-1 Shikata-cho Kita Ward, Okayama 700-8558, Japan.

Phone: +81-86-235-7227

Fax: +81-86-232-8226

E-mail: kohashi@cc.okayama-u.ac.jp

Conflicts of interest

All authors declare no conflicts of interest regarding this study.

Abbreviations

ALK, anaplastic lymphoma kinase; AREG, amphiregulin; EGFR, epidermal growth factor receptor; EML4, echinoderm microtubule-associated protein-like 4; FISH, fluorescence *in situ* hybridization; MET, MET proto-oncogene receptor tyrosine kinase; MRI, magnetic resonance imaging; NOG, NOD/Shi-scid/IL-2Rγ^{null}; NSCLC, non-small cell lung cancer; NGS, next-generation sequencing; PARP1, poly(ADP-ribose) polymerase 1; PDX, patient-derived xenograft; PFS, progression-free survival; POLE, DNA polymerase epsilon; TKI, tyrosine kinase inhibitor; TMB, tumor mutation burden

Abstract

Introduction: The highly selective ALK inhibitor alectinib is standard therapy for *ALK*-positive lung cancers; however, some tumors quickly develop resistance. Here, we investigated the mechanism associated with rapid acquisition of resistance using clinical samples.

Methods: Autopsied samples were obtained from lung, liver, and renal tumors from a 51-year-old male patient with advanced *ALK*-positive lung cancer and who had acquired resistance to alectinib in only 3 months. We established an alectinib-resistant cell line (ABC-14) from pleural effusion and an alectinib/crizotinib-resistant cell line (ABC-17) and patient-derived xenograft (PDX) model from liver tumors. Additionally, we performed next-generation sequencing (NGS), direct DNA sequencing, and quantitative real-time reverse-transcription polymerase chain reaction.

Results: ABC-14 cells harbored no *ALK* mutations and were sensitive to crizotinib while also exhibiting *MET* gene amplification and *amphiregulin* overexpression. Additionally, combined treatment with crizotinib/erlotinib inhibited cell growth. ABC-17 and PDX tumors harbored *ALK G1202R*, and PDX tumors metastasized to multiple organs *in vivo*, whereas the third generation ALK-inhibitor, lorlatinib, diminished tumor growth *in vitro* and *in vivo*. NGS indicated high tumor mutation burden (TMB) and heterogeneous tumor evolution. The autopsied lung tumors harbored *ALK G1202R* (c. 3604 G>A) and the right renal metastasis harbored *ALK G1202R* (c. 3604 G>C); the mutation thus comprised different codon changes.

Conclusions: High TMB and heterogeneous tumor evolution might be responsible for rapid acquisition of alectinib resistance. Timely lorlatinib administration or combined therapy with an ALK inhibitor and other receptor tyrosine-kinase inhibitors might constitute a potent strategy.

Keywords: NSCLC, alectinib, ALK G1202R, MET, amphiregulin

Introduction

Molecular therapies targeting gene alterations of driver oncogenes, such as *epidermal growth factor receptor* (*EGFR*) or *anaplastic lymphoma kinase* (*ALK*), are standard treatment strategies for advanced non-small cell lung cancer (NSCLC).[1] The second-generation ALK inhibitor alectinib shows a high objective response rate (93.5%) and a long progression-free survival (PFS) rate (3-year PFS: 62%) for *ALK*-positive NSCLC[2]; however, a portion of patients rapidly acquire resistance to alectinib within 3 months.[3, 4]

To date, several mechanisms of resistance to alectinib, such as *ALK* mutations, have been reported in clinical samples. Resistance mutations in the ALK kinase domain, such as G1202R, are more frequently detected in tumors treated with alectinib (29%) relative to those treated with crizotinib (2%)[5]; however, the mechanisms underlying this rapid acquisition of resistance to alectinib have yet to be clarified.

Here, we investigated the mechanism associated with rapid acquisition of resistance to alectinib using patient-derived samples, including autopsied tissues. All samples were collected from a single patient with NSCLC harboring *echinoderm microtubule-associated protein-like 4* (*EML4*)-*ALK* fusion genes and who responded to alectinib immediately as an initial treatment, albeit quickly acquired resistance. We comprehensively analyzed multiple clinical samples of pre- and post-alectinib treatment using next-generation sequencing (NGS) and performed *in vitro* and *in vivo* experiments using novel cell lines or a patient-derived xenograft (PDX) model.

Materials and Methods

Detailed information is provided in the Supplementary Information.

In vitro experiments and xenograft models

Cell culture, western blot, and immunohistochemistry were performed, as previously described.[6] The animal experimental protocol was approved by the Animal Care and Use Committee, Okayama University (Okayama, Japan) (OKU-2017084, 2017085).

NGS and tumor mutation burden (TMB) analysis

cDNA libraries were prepared using the TruSeq RNA Access library prep kit (Illumina, San Diego, CA, USA), and RNA sequencing was performed on a HiSeq sequencing system (Illumina). An unrooted phylogenetic tree was analyzed and displayed using the hclust, as.phylo, and plot functions under the RStudio environment (https://www.rstudio.com/). TMB was calculated for the selected 341 genes using MSK-IMPACT version 1.0 according to a previous report.[7]

Results

Clinical course of the patient and sample collection

A 51-year-old male patient (ex-smoker; 32 pack years) with no history of prior malignancies or radiation or chemotherapy was hospitalized in the coronary care unit due to pericardial effusion and acute heart failure (Fig. 1A). Computed tomography detected right-middle lung tumors with bilateral plural effusion and multiple liver tumors. Brain magnetic resonance imaging (MRI) showed metastatic lesions (Supplementary Fig. S1), and after drainage of the pericardial effusion, transbronchial biopsy of the primary lung tumor revealed adenocarcinoma with upregulated levels of the ALK protein and *ALK* translocation confirmed by fluorescence *in situ* hybridization (FISH) (Fig. 1B and Supplementary Fig. S2A). Alectinib (600 mg/day) inhibited lung tumor growth according to Response Evaluation Criteria in Solid Tumor version 1.1 criteria describing partial response (RECIST PR) (Supplementary Table S1), and the patient was discharged from the hospital 20 days after alectinib administration. However, metastatic liver tumors quickly regrew only 3 months later (Fig. 1C). After four cycles of administration of cisplatin (75 mg/m^2) plus pemetrexed (500 mg/m^2), followed by two cycles of maintenance therapy with pemetrexed (best overall response: RECIST PR) (Supplementary Table S2), another ALK inhibitor, ceritinib (750 mg/day), was administrated for 1 month but showed little effect on tumor growth and was accompanied by intolerable toxicity (Supplementary Table S3). Crizotinib (500 mg/day) was then administered, resulting in slightly reductions in the pleural effusion but lymphangitic carcinomatosis of the right lung, although progression of multiple liver metastases was observed. The small brain metastases identified in the temporal lobe and parietal lobe at diagnosis improved after 1.5 months of alectinib treatment. Prior to initiating ceritinib therapy, the metastases regrew; however, after ceritinib therapy, these lesions were not clear in the brain MRI image (Supplementary Fig. S1). The patient survived with lung cancer for only 12 months, and an autopsy was performed following family consent. The blood

sample for circulating tumor DNA analysis could not be obtained during the clinical course.

We established two cell lines: the first (ABC-14) from pleural effusion and the other (ABC-17) from PDX tumors from liver lesions generated using NOD/Shi-scid/IL-2Rγ^{null} (NOG) mice (Fig. 1A and Supplementary Fig. S2B). The *ALK* fusion gene and upregulated levels of the ALK protein were confirmed in ABC-14, ABC-17, PDX tumors, and all autopsy specimens (lung, liver, and kidney) by immunohistochemistry or direct sequencing (Fig. 1B and Supplementary Fig. S2C). A common *B-cell lymphoma-2*-like 11-gene deletion, known as an intrinsic resistance mechanism to tyrosine kinase inhibitors (TKIs), was not found in either the ABC-14 or ABC-17 cell line (Supplementary Figs. S3A and B).[8]

Activation of EGFR/MET signaling in ABC-14 cells and presence of the *ALK* mutation resulting in the G1202R substitution in ABC-17 cells

Consistent with the clinical course, alectinib had limited inhibitory effect on *in vitro* cell proliferation (Figs. 2A and 3A) and the phosphorylation of ALK, signal transducer and activator of transcription 3 (STAT3), AKT, and extracellular signal-regulated kinase (ERK)1/2 (Figs. 2B and 3B) in ABC-14 and ABC-17 cells. NGS suggested that mRNA levels of *MET proto-oncogene receptor tyrosine kinase (MET)* and the EGFR ligand *amphiregulin AREG* were elevated in ABC-14 cells (Supplementary Fig. S4A), with *MET* amplification confirmed by FISH (*MET*/*CEP7* ratio, 5.6) and MET activation confirmed at the protein level (Figs. 2C and D; Supplementary Figs. S5A and B). Additionally, we confirmed increased AREG secretion (Fig. 2E). Consistently, we observed the synergistic effect of combined therapy with the ALK/MET inhibitor crizotinib and the EGFR TKI erlotinib or triple therapy with alectinib, erlotinib, and the MET inhibitor SGX-523 in ABC-14 cells *in vitro* and *in vivo* (Figs. 2F–H and Supplementary Fig. S5D).

NGS and direct sequencing of the ALK kinase domain revealed that both ABC-17 cells and

PDX tumors harbored a point mutation (G1202R) (Fig. 3C and Supplementary Fig. S4B). Moreover, we found that ABC-17 cells did not display elevated *MET* expression or MET protein levels, and that MET phosphorylation was also not activated (Supplementary Fig. S5C). As previously reported,[9] lorlatinib treatment strongly inhibited cell proliferation *in vitro* (IC_{50} = 65 nM) ALK, STAT3, AKT, and ERK1/2 phosphorylation in ABC-17 cells (Figs. 3D and E). Furthermore, lorlatinib treatment showed much stronger effects in ABC-17 tumors as compared with alectinib or crizotinib treatment *in vivo* (Fig. 3F).

Lorlatinib diminishes PDX tumors with metastatic capability in NOG mice

We then analyzed the metastatic capability of tumors in the PDX model using NOG mice. Interestingly, 10 weeks after tumor injection, mice developed multiple metastatic lesions in the lung, liver, spleen, and adrenal gland (Figs. 4A and B). Metastatic lesions were more frequently detected in PDX mice as compared with those in NOG mice xenografted using ABC-14 or ABC-17 cells (Fig. 4C).

The epithelial-to-mesenchymal transition reportedly plays a role in the metastatic ability of cancer cells.[10] We found that ABC-17 cells showed decreased E-cadherin and increased vimentin levels (Supplementary Figs. S6A and B), and that compared with ABC-17 cells, PDX tumors or tissue from autopsied liver metastatic lesions contained fewer vimentin-positive cells (Supplementary Figs. S4A, S6A, and S6B), whereas vimentin was observed in stromal cells from PDX tumors. A previous study suggested that vimentin-positive stromal cells might potentially affect metastatic ability.[11] We then determined the efficacy of lorlatinib treatment in PDX tumors, finding that lorlatinib diminished tumor growth and lung metastasis almost completely without loss of body weight, whereas neither alectinib nor crizotinib treatment showed any effect on tumor growth or metastatic ability (Fig. 4D).

Heterogeneous tumor evolution and high TMB

A recent study revealed that TMB negatively affects the duration of treatment with driver oncoprotein inhibitors.[12] Based on this finding, we assessed TMB in our samples using a previously described process[7] by calculating TMB using 341 genes included in MSK-IMPACT version 1.0. Briefly, we extracted the number of mutations in the selected genes from NGS data, and TMB was calculated by dividing the number of mutations by the total genomic area where the mutations were reported (0.98 Mb), with the threshold for high TMB defined as >13.8 mutations/Mb. Interestingly, pretreatment samples and autopsied tumors showed high TMB (≥25 mutations/Mb) (Fig. 5A). Moreover, the mutation pattern did not indicate a smoking signature (Supplementary Table. S4 and S5), microsatellite regions were stable, and we detected no mutation of DNA polymerase epsilon (POLE) or defects in genes associated with DNA-damage repair (DDR), although expression levels of some DDR genes, such as *poly(ADP-ribose) polymerase 1* (*PARP1*) and *X-ray repair cross-complementing 1*, were elevated (Supplementary Fig. S7A).

We then assessed the evolution of the resistant tumors. The *EML4-ALK* fusion (variant 3a/3b) was confirmed in all samples (Supplementary Fig. S2C), with mRNA-expression profiles varying between pretreatment samples and post-treatment autopsied samples (Supplementary Figs. S7B, 7C). These results might suggest that the tumor evolved heterogeneously. The *ALK* mutation resulting in the G1202R substitution and resistance was detected in ABC-17 cells, PDX tumors, as well as autopsied liver samples, right middle lung tumors, and right renal tumors; however, it was not detected in ABC-14 cells, the plural effusion from which the ABC-14 cells was derived, or left renal tumors (Supplementary Figs. S4B–D, S8A and S8B). This result suggested that cancer cells harboring the ALK G1202R mutation existed heterogeneously in each metastatic site. Additionally, we found that the associated *ALK* mutations comprised different codon changes at different sites (i.e., primary

lung: GGA to AGA; right renal metastasis: GGA to CGA) (Fig. 5B). Other types of secondary *ALK* mutation were not detected.

Consequently, these data suggested that the *ALK*-positive lung cancer tumors displayed high TMB and evolved in various ways, and that heterogeneous drug-resistant clones existed in the same patient.

Discussion

Development of alternative treatment strategies for cases of rapid alectinib resistance represents an important clinical issue for lung cancers harboring *ALK* fusions. This study revealed the following major findings: 1) several resistant mechanisms, including activation of MET, EGFR, or resistant ALK G1202R mutation, can occur in the same patient (Supplementary Figs. 9A and B); 2) ALK G1202R was heterogeneously detected among autopsied samples, with this mutation the result of different codon changes (Fig. 5B); and 3) the tumors showed high TMB and heterogonous tumor evolution.

Lung cancers with *ALK* fusions exhibit high diversity[13]; therefore, some patients might benefit from treatment with alectinib alone, whereas others, such as the patient described in the present study, might require other-generation ALK inhibitors or intensive combination therapies. It is possible that shifting of the therapeutic regimen to lorlatinib or a combination therapy at an appropriate time might have changed the outcome of the present case. In the future, it might be possible to select a suitable treatment strategy based on liquid-biopsy-based gene profiling.[14]

Pretreatment samples showed high TMB, indicating that the tumors might have exhibited genome instability. A recent study reported correlations between high TMB and high microsatellite instability, POLE mutation, or defective DDR genes,[15-17] none of which were detected in our case. Another study reported overexpression of DDR genes, including

PARP1 generated DNA repair error.[18] Although the precise mechanism remains unknown, such genome instability might have existed, which could have induced the heterogeneous evolution. Consistently, we observed several mechanisms of resistance, with the ALK G1202R mutation identified among samples resulting from different codon changes. The heterogeneous evolution of the tumors and the multiple mechanisms of resistance might be the main factors underlying the rapid development of resistance.

In conclusion, we comprehensively analyzed samples derived from a patient with rapidly acquired resistance to alectinib. Timely administration of next-generation ALK inhibitors or combination therapies could be an effective alternative treatment strategy for drug-resistant lung cancers. Further studies are warranted involving patients with lung cancer harboring *ALK* fusion genes and displaying rapidly acquired resistance to alectinib.

Acknowledgements

First, we thank the patient and his family. We are grateful to Hiromi Nakashima and Kyoko Maeda for the technical support and thank our laboratory colleagues for the useful discussions. Additionally, we thank Editage (www.editage.jp) for help with English-language editing.

References

1. Soda M, Choi YL, Enomoto M, et al. Identification of the transforming EML4-ALK fusion gene in non-small-cell lung cancer. *Nature* 2007;448:561-566.

2. Tamura T, Kiura K, Seto T, et al. Three-Year Follow-Up of an Alectinib Phase I/II Study in ALK-Positive Non-Small-Cell Lung Cancer: AF-001JP. *J Clin Oncol* 2017;35:1515-1521.

3. Hida T, Nokihara H, Kondo M, et al. Alectinib versus crizotinib in patients with ALK-positive non-small-cell lung cancer (J-ALEX): an open-label, randomised phase 3 trial. *Lancet* 2017;390:29-39.

4. Peters S, Camidge DR, Shaw AT, et al. Alectinib versus Crizotinib in Untreated ALK-Positive Non-Small-Cell Lung Cancer. *N Engl J Med* 2017;377:829-838.

5. Gainor JF, Dardaei L, Yoda S, et al. Molecular Mechanisms of Resistance to First- and Second-Generation ALK Inhibitors in ALK-Rearranged Lung Cancer. *Cancer Discov* 2016;6:1118-1133.

6. Ninomiya K, Ohashi K, Makimoto G, et al. MET or NRAS amplification is an acquired resistance mechanism to the third-generation EGFR inhibitor naquotinib. *Sci Rep* 2018;8:1955.

7. Zehir A, Benayed R, Shah RH, et al. Mutational landscape of metastatic cancer revealed from prospective clinical sequencing of 10,000 patients. *Nat Med* 2017;23:703-713.

8. Ng KP, Hillmer AM, Chuah CT, et al. A common BIM deletion polymorphism mediates intrinsic resistance and inferior responses to tyrosine kinase inhibitors in cancer. *Nat Med* 2012;18:521-528.

9. Zou HY, Friboulet L, Kodack DP, et al. PF-06463922, an ALK/ROS1 Inhibitor, Overcomes Resistance to First and Second Generation ALK Inhibitors in Preclinical Models. *Cancer Cell* 2015;28:70-81.

10. Yeung KT, Yang J. Epithelial-mesenchymal transition in tumor metastasis. *Mol Oncol* 2017;11:28-39.

11. Richardson AM, Havel LS, Koyen AE, et al. Vimentin Is Required for Lung Adenocarcinoma Metastasis via Heterotypic Tumor Cell-Cancer-Associated Fibroblast Interactions during Collective Invasion. *Clin Cancer Res* 2018;24:420-432.

12. Offin M, Rizvi H, Tenet M, et al. Tumor Mutation Burden and Efficacy of EGFR-Tyrosine Kinase Inhibitors in Patients with EGFR-Mutant Lung Cancers. *Clin Cancer Res* 2019;25:1063-1069.

13. Yoshida T, Oya Y, Tanaka K, et al. Differential Crizotinib Response Duration Among ALK Fusion Variants in ALK-Positive Non-Small-Cell Lung Cancer. *J Clin Oncol* 2016;34:3383-3389.

14. Dagogo-Jack I, Brannon AR, Ferris LA, et al. Tracking the Evolution of Resistance to ALK Tyrosine Kinase Inhibitors through Longitudinal Analysis of Circulating Tumor DNA. *JCO Precis Oncol* 2018 (in press).

15. Chalmers ZR, Connelly CF, Fabrizio D, et al. Analysis of 100,000 human cancer genomes reveals the landscape of tumor mutational burden. *Genome Med* 2017;9:34.

16. Hatakeyama K, Nagashima T, Ohshima K, et al. Mutational burden and signatures in 4000 Japanese cancers provide insights into tumorigenesis and response to therapy. *Cancer Sci* 2019 (in press).
17. Parikh AR, He Y, Hong TS, et al. Analysis of DNA Damage Response Gene Alterations and Tumor Mutational Burden Across 17,486 Tubular Gastrointestinal Carcinomas: Implications for Therapy. *Oncologist* 2019 (in press).
18. Muvarak N, Kelley S, Robert C, et al. c-MYC Generates Repair Errors via Increased Transcription of Alternative-NHEJ Factors, LIG3 and PARP1, in Tyrosine Kinase-Activated Leukemias. *Mol Cancer Res* 2015;13:699-712.

Figure 1. Patient clinical course and establishment of the ABC-14 and ABC-17 cell lines and the PDX model. **A,** Clinical course of the patient harboring *EML4-ALK*-positive lung adenocarcinoma. **B,** Immunohistochemistry targeting ALK in the established cell lines (ABC-14 and ABC-17) and autopsy samples (primary tumors, liver, bilateral kidney, and PDX tumor). Scale bar: 50 μm. **C,** Computed tomography images of the patient: i) before first-line treatment with alectinib, ii) 1 month after initiation of alectinib treatment, and iii) 3 months after alectinib treatment. Lung primary lesions (top) and liver metastases (bottom). Alec, alectinib; ALK, anaplastic lymphoma kinase; EML4, echinoderm microtubule-associated protein-like 4; CDDP, cisplatin; Ceri, ceritinib; Criz, crizotinib; meta, metastasis; PDX, patient-derived xenograft; PEM, pemetrexed.

Figure 2. Resistance mechanism of the established ABC-14 cell line. **A,** MTT assays following treatment of ABC-14 cells with the indicated concentrations of alectinib and crizotinib. Error bars indicate standard error. All experiments were performed in triplicate. **B,** Effect of alectinib or crizotinib treatment on survival signaling in ABC-14 cells. ABC-14 cells were left untreated or incubated with alectinib (1, 10, 10^2, 10^3, or 10^4 nM) or crizotinib (1, 10, 10^2, 10^3, or 10^4 nM) for 4 h. Lysates were analyzed by western blot. **C,** FISH analysis of *MET* amplification in ABC-14 cells. Red, *MET* gene; green, *CEP7* gene. *MET/CEP7* ratio, 5.6. **D,** Phospho-receptor tyrosine kinase arrays for ABC-14 cells. **E,** AREG concentrations in culture medium. Viable supernatant was assessed by enzyme-linked immunosorbent assay. Error bars represent the standard error. *$P < 0.01$. **F,** Inhibitory effect of combined therapy with ALK inhibitors (500 nM), an EGFR TKI, and MET inhibitors (1.0 μM, respectively) on the proliferation of ABC-14 cells (MTT assay) over 96 h. Data represent the mean ± standard error of the mean of three independent experiments. *$P < 0.01$. ALK inhibitors; alectinib and crizotinib; MET inhibitors; crizotinib and SGX-523; EGFR TKI; erlotinib. **G,** Inhibitory effect of combined therapy with

ALK inhibitors, an EGFR TKI, and MET inhibitors on survival signaling in ABC-14 cells. Cells were left untreated or incubated with alectinib (500 nM) or crizotinib (500 nM) in the presence or absence of erlotinib (1.0 μM) or SGX-523 (1.0 μM) for 4 h. Lysates were analyzed by western blot. **H,** Effect of combined therapy with crizotinib and erlotinib on tumor growth and body weight in xenograft models. ABC-14 xenograft tumors were treated with 50 mg/kg/day crizotinib or 25 mg/kg/day erlotinib or combination therapy, respectively. Data from vehicle and treated groups were statistically analyzed on day 29. Error bars represent the standard error. Curves represent tumor volume (top) and body weight (bottom). $*P < 0.05$.
ALK, anaplastic lymphoma kinase; AREG, amphiregulin; EGFR, epidermal growth factor receptor; FISH, fluorescence *in situ* hybridization; MET, MET proto-oncogene receptor tyrosine kinase; TKI, tyrosine kinase inhibitor

Figure 3. Resistance mechanism of the established ABC-17 cell line. **A,** MTT assays following treatment of ABC-17 cells with the indicated concentrations of alectinib and crizotinib. H3122 is a cell line sensitive to alectinib and crizotinib. Error bars represent the standard error. All experiments were performed in triplicate. **B,** Effect of alectinib or crizotinib on survival signaling in ABC-17 cells. Cells were left untreated or incubated with alectinib (1, 10, 10^2, 10^3, or 10^4 nM) or crizotinib (1, 10, 10^2, 10^3, or 10^4 nM) for 4 h. Lysates were analyzed by western blot. **C,** Direct sequencing of the ALK kinase domain in ABC-14 and ABC-17 cells. **D,** MTT assays following treatment of ABC-17 cells with the indicated concentrations of lorlatinib. Error bars represent the standard error. All experiments were performed in triplicate. **E,** Effect of lorlatinib on survival signaling in ABC-14 and ABC-17 cells. Both lines were left untreated or incubated with lorlatinib (1, 10, 10^2, 10^3, or 10^4 nM) for 4 h. Lysates were analyzed by western blot. **F,** Effects of ALK inhibitors on tumor growth and body weight in xenograft models. ABC-17 xenograft tumors were treated with 10 mg/kg/day alectinib, 50 mg/kg/day

crizotinib, or 10 mg/kg/day lorlatinib. Data for vehicle and treated groups were statistically analyzed on day 29. Error bars represent the standard error. Curves represent tumor volume (top) and body weight (bottom). *$P < 0.05$.

ALK, anaplastic lymphoma kinase.

Figure 4. Metastatic features and drug sensitivity in PDX model mice. **A,** Autopsy findings from the PDX model mice. PDX tumors were passaged subcutaneously between NOG mice, and mice were sacrificed at 10 weeks after subcutaneous tumor injection. **B,** Various tumor lesions were stained with hematoxylin and eosin (left) or for immunohistochemistry targeting ALK (right). Short bars: 500 μm; long bars: 50 μm. **C,** Metastatic lesions in various xenograft types. A total of 5×10^6 ABC-14 cells, ABC-17 cells, or PDX tumor cells were injected subcutaneously into mice, followed by sacrifice at 10-weeks post-injection and lesion assessment, including counting. **D,** Effects of ALK inhibitors on tumor growth and body weight in xenograft models. PDX tumors were treated with 10 mg/kg/day alectinib, 50 mg/kg/day crizotinib, or 10 mg/kg/day lorlatinib. Data from vehicle and treated groups were statistically analyzed on day 29. Error bars represent the standard error. Curves represent tumor volume (top) and body weight (bottom). *$P < 0.05$.

ALK, anaplastic lymphoma kinase; PDX, patient-derived xenograft.

Figure 5. Comprehensive analysis of established cell lines, PDX model tumors, and clinical autopsy samples by RNA sequencing. **A,** Tumor mutation burden calculated using RNA-sequencing data from clinical samples and established cell lines. Normal lung tissues were obtained from other patients who underwent surgical resection for lung cancers.

B, Summary of the gene characteristics of autopsied specimens.

Autopsy lung, autopsied sample from the right lung tumor; lt, left; meta, metastatic lesion; rt,

right; PDX, patient-derived xenograft.

Supplemental Data 1. Pdf

Supplemental Data 2. docx

Figure 1

A

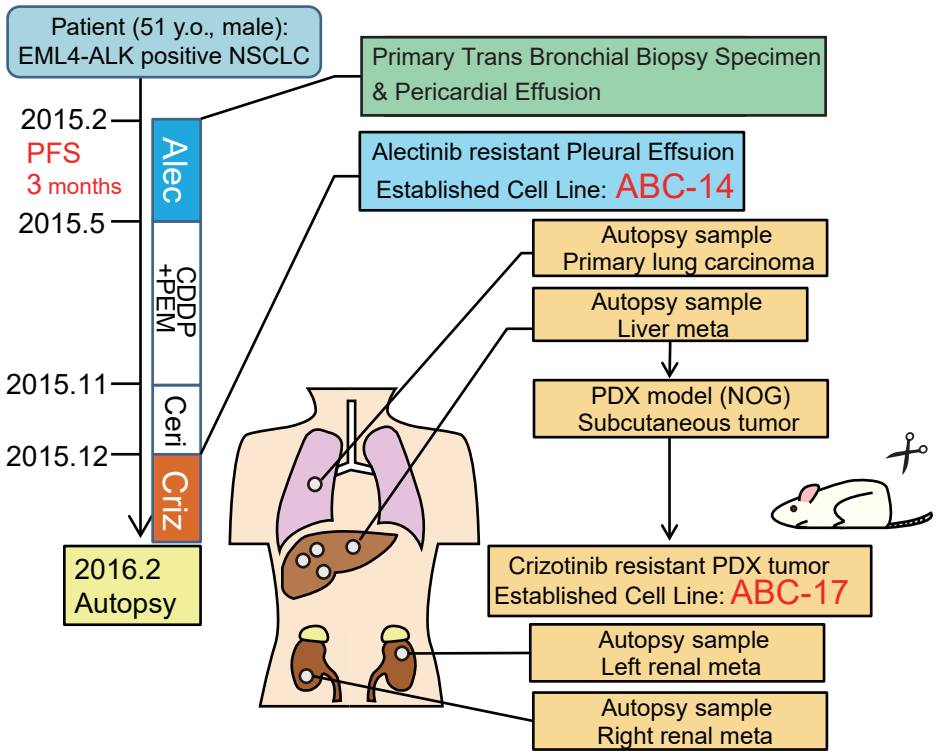
Patient (51 y.o., male):
EML4-ALK positive NSCLC
Primary Trans Bronchial Biopsy Specimen
& Pericardial Effusion
2015.2
PFS
3 months
2015.5
2015.11
2015.12
Alec
CDDP
+PEM
Ceri
Criz
Alectinib resistant Pleural Effsuion
Established Cell Line: ABC-14
Autopsy sample
Primary lung carcinoma
Autopsy sample
Liver meta
PDX model (NOG)
Subcutaneous tumor
2016.2
Autopsy
Crizotinib resistant PDX tumor
Established Cell Line: ABC-17
Autopsy sample
Left renal meta
Autopsy sample
Right renal meta

B

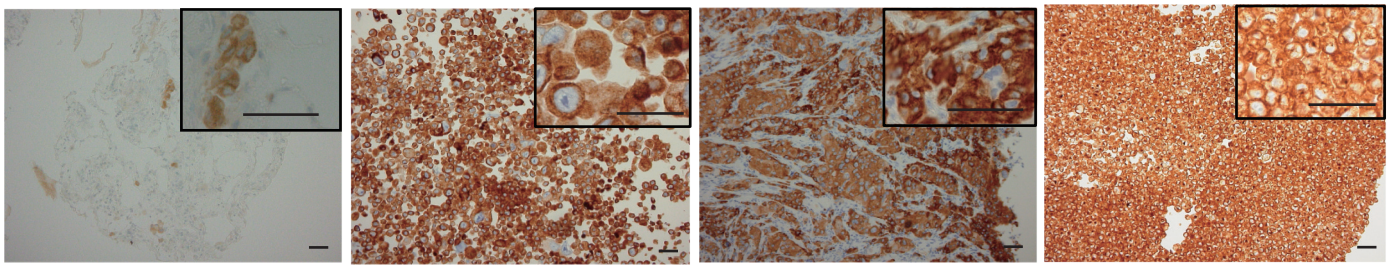
Primary tumors
ABC-14
PDX 3rd tumor
ABC-17

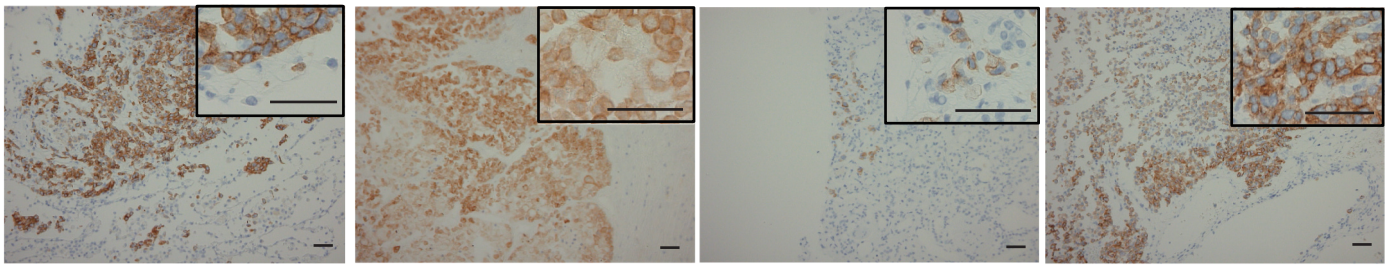
Autopsy primary tumors
Autopsy liver meta
Autopsy left renal meta
Autopsy right renal meta

C

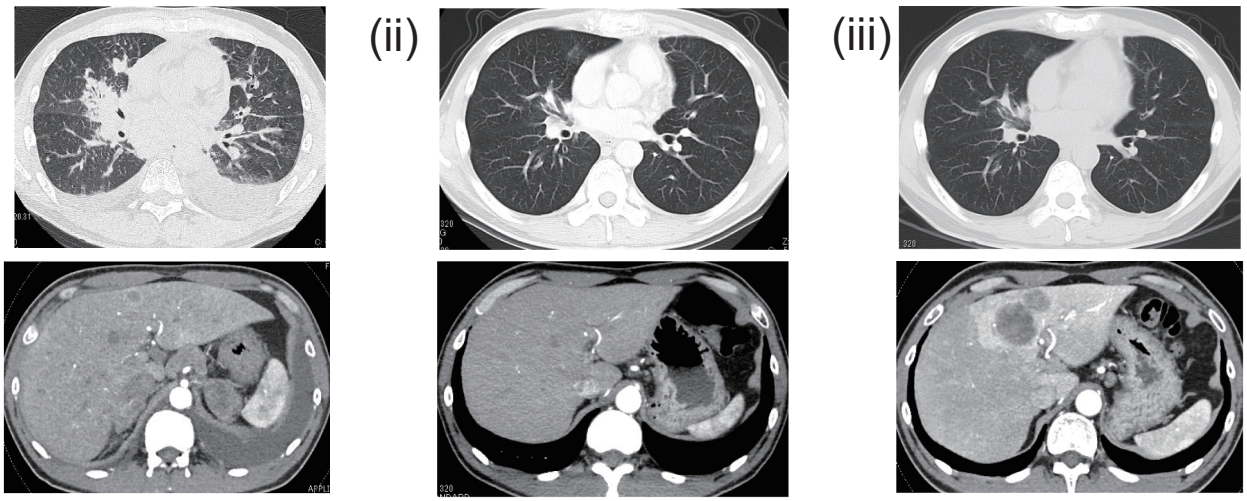
(i)
(ii)
(iii)

Figure 2

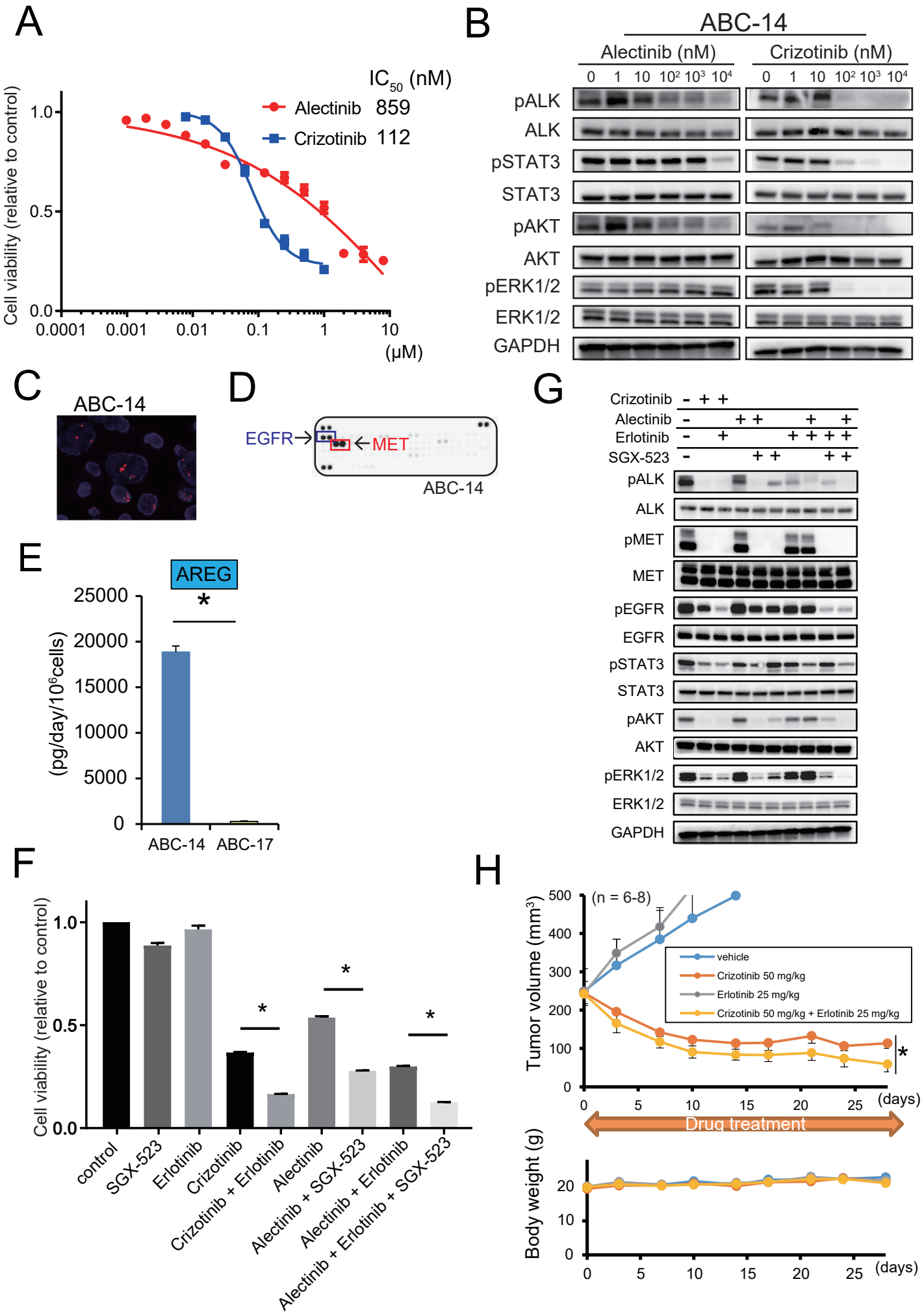
A
IC50 (nM)
Alectinib 859
Crizotinib 112
Cell viability (relative to control)
1.0
0.5
0.0
0.0001
0.001
0.01
0.1
1
10
(μM)
B
ABC-14
Alectinib (nM)
Crizotinib (nM)
0 1 10 10² 10³ 10⁴
0 1 10 10² 10³ 10⁴
pALK
ALK
pSTAT3
STAT3
pAKT
AKT
pERK1/2
ERK1/2
GAPDH
C
ABC-14
D
EGFR
MET
ABC-14
E
AREG
*
25000
20000
15000
10000
5000
0
(pg/day/10⁶cells)
ABC-14
ABC-17
F
Cell viability (relative to control)
1.0
0.5
0.0
*
*
*
control
SGX-523
Erlotinib
Crizotinib
Crizotinib + Erlotinib
Alectinib
Alectinib + SGX-523
Alectinib + Erlotinib
Alectinib + Erlotinib + SGX-523
G
Crizotinib - + +
Alectinib - + + + +
Erlotinib - + + + + +
SGX-523 - + + + +
pALK
ALK
pMET
MET
pEGFR
EGFR
pSTAT3
STAT3
pAKT
AKT
pERK1/2
ERK1/2
GAPDH
H
(n = 6-8)
Tumor volume (mm³)
500
400
300
200
100
0
vehicle
Crizotinib 50 mg/kg
Erlotinib 25 mg/kg
Crizotinib 50 mg/kg + Erlotinib 25 mg/kg
*
0 5 10 15 20 25 (days)
Drug treatment
Body weight (g)
20
10
0
0 5 10 15 20 25 (days)

Figure 3

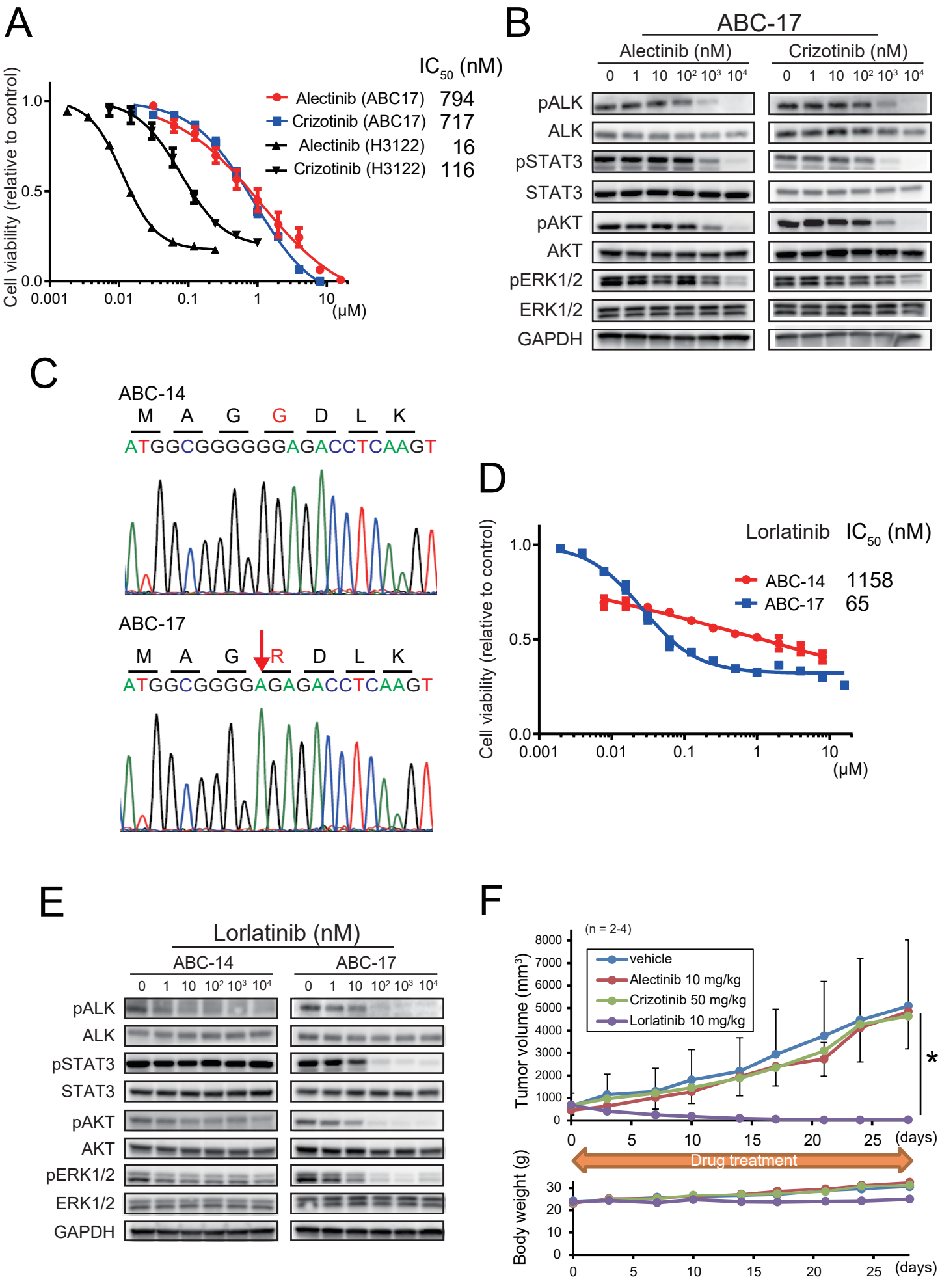
A
IC50 (nM)
Alectinib (ABC17) 794
Crizotinib (ABC17) 717
Alectinib (H3122) 16
Crizotinib (H3122) 116
Cell viability (relative to control)
1.0
0.5
0.0
0.001
0.01
0.1
1
10
(μM)
B
ABC-17
Alectinib (nM)
Crizotinib (nM)
0 1 10 10² 10³ 10⁴
pALK
ALK
pSTAT3
STAT3
pAKT
AKT
pERK1/2
ERK1/2
GAPDH
C
ABC-14
M A G G D L K
ATGGCGGGGGGAGACCTCAAGT
ABC-17
M A G R D L K
ATGGCGGGGAGAGACCTCAAGT
D
Lorlatinib IC50 (nM)
ABC-14 1158
ABC-17 65
Cell viability (relative to control)
1.0
0.5
0.0
0.001
0.01
0.1
1
10
(μM)
E
Lorlatinib (nM)
ABC-14
ABC-17
0 1 10 10² 10³ 10⁴
pALK
ALK
pSTAT3
STAT3
pAKT
AKT
pERK1/2
ERK1/2
GAPDH
F
(n = 2-4)
vehicle
Alectinib 10 mg/kg
Crizotinib 50 mg/kg
Lorlatinib 10 mg/kg
Tumor volume (mm³)
8000
7000
6000
5000
4000
3000
2000
1000
0
0 5 10 15 20 25 (days)
*
Drug treatment
Body weight (g)
30
20
10
0
0 5 10 15 20 25 (days)

Figure 4

A

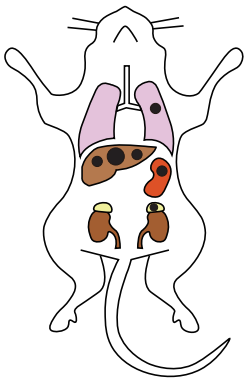

C

	MetstaticLesion				
Type of cancer cells	Lung	Liver	Spleen	Adrenal gland	Others
ABC-14	3/3	0/3	0/3	0/3	
ABC-17	1/3	0/3	0/3	0/3	
PDX	9/9	2/9	2/9	2/9	Peritoneum, Axilla LN

B

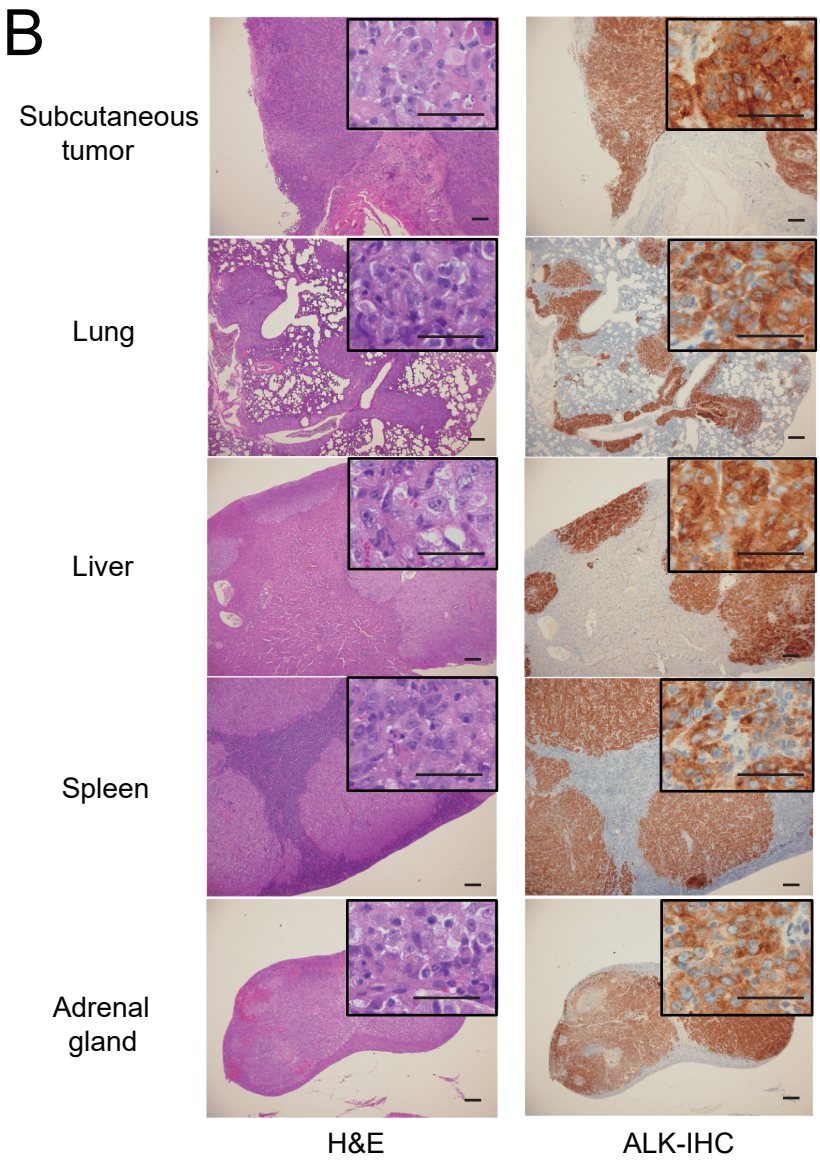

D

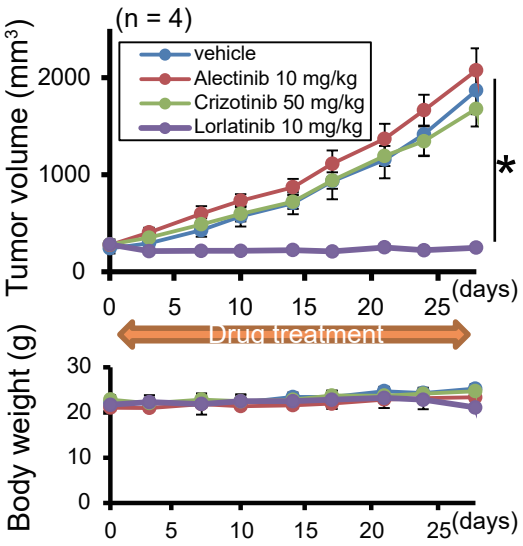

	Vehicle	Alectinib	Crizotinib	Lorlatinib
Lung meta	2/2	2/2	2/2	0/2

Figure 5

A

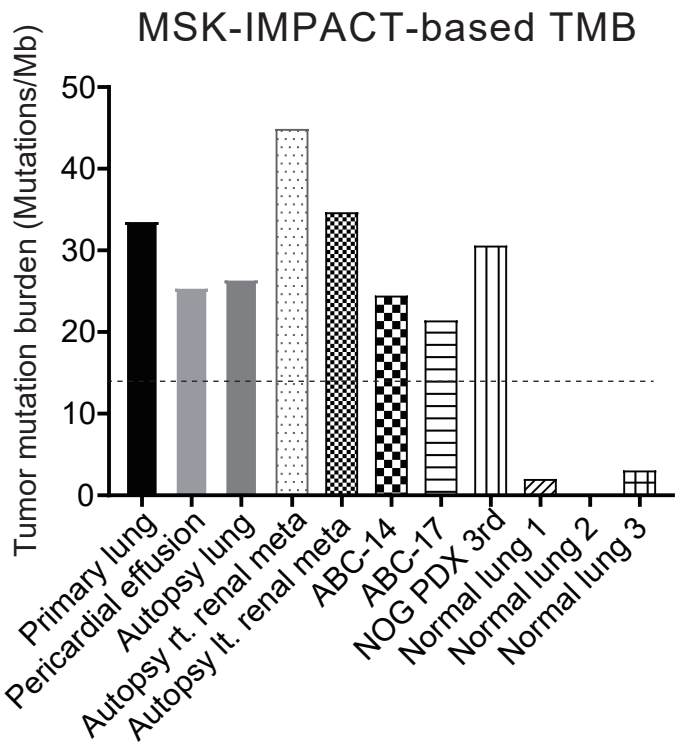
MSK-IMPACT-based TMB
Tumor mutation burden (Mutations/Mb)
50
40
30
20
10
0
Primary lung
Pericardial effusion
Autopsy lung
Autopsy rt. renal meta
Autopsy lt. renal meta
ABC-14
ABC-17
NOG PDX 3rd
Normal lung 1
Normal lung 2
Normal lung 3

B

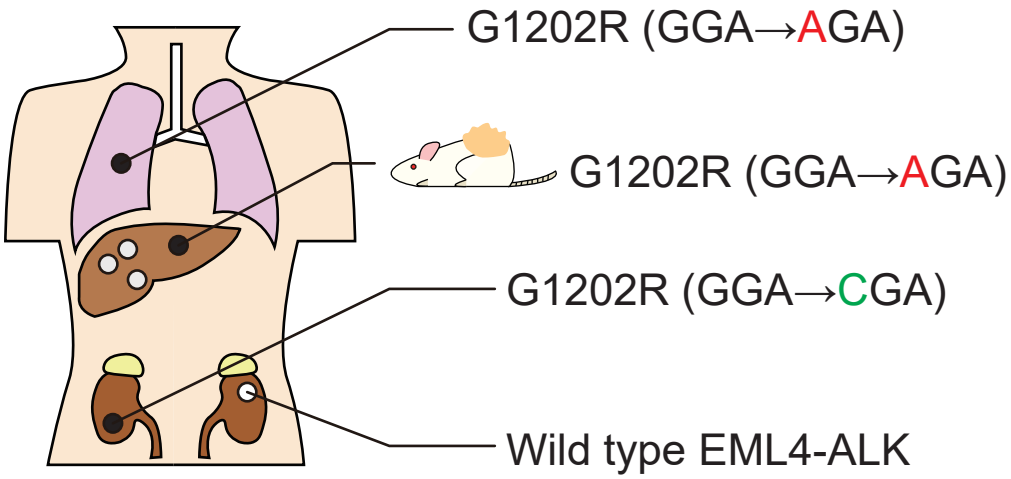
G1202R (GGA→AGA)
G1202R (GGA→AGA)
G1202R (GGA→CGA)
Wild type EML4-ALK

Supplementary Materials and Methods

Cell lines and reagents

PC-9 cells (epidermal growth factor receptor: *EGFR Ex19 del E746_A750*) were purchased from the European Collection of Authenticated Cell Cultures in 2014 (Catalogue No.: 90071810). 293T cells were purchased from RIKEN Cell Bank in 2016 (Resource No.: RBRC-RCB2202). H3122 cells (EML4-ALK variant 1 E13; A20) were kindly provided by Dr. William Pao (Vanderbilt University, Nashville, TN, USA) in 2012. Cell lines were resuscitated at least every 3 months from frozen master stocks.

ABC-14 and ABC-17 cell lines were established at Okayama University Hospital from 51-y.o. male patient with EML4-ALK-positive NSCLC in 2016. ABC-14 was established from pleural effusion following alectinib therapy (Fig. 1A) as described previously[1]. Numerous tumor clusters were observed cytologically in the effusion. Mononuclear cells were isolated from the malignant effusion using the Ficoll–Hypaque method and washed twice with RPMI-1640 medium. The cells were suspended in a 6-well dish with RPMI-1640 medium supplemented with 10% fetal bovine serum and 1% penicillin/streptomycin and began growing within several weeks and proliferated consistently thereafter. ABC-17 was derived from PDX tumors, which were established from a liver metastatic tumor harvested upon autopsy (Fig. 1A). The liver metastasis sample was minced and injected subcutaneously into the back of a female NOG mouse (NOD/Shi-scid, IL-2RγKO Jic) purchased at 6 weeks of age from In-Vivo Science, Japan for the PDX model. Two months after the injection without drug treatment, the subcutaneous tumor grew up and was minced and washed twice with RPMI 1640 medium. To eliminate mouse fibroblast cells and establish the purified tumor cell line, ABC-17, we used the Mouse Cell Depletion Kit (Miltenyi Biotec, Auburn, CA, USA) according to the manufacturer's protocol.

PDX tumors were homogenized using the Tumor Dissociation Kit, human (Cat. No. 130-095-929, Miltenyi Biotec) and transplanted from mouse to mouse by injecting homogenized cells subcutaneously into the backs of the mice. Written informed consent was obtained from the patient and his family and the Institutional Review Board of Okayama University approved this experiment (approval no. 1603-066). The animal experimental protocol was approved by the Animal Care and Use Committee, Okayama University, Okayama, Japan (OKU-2017085). Cells were cultured in RPMI 1640 medium supplemented with 10% heat-inactivated FBS and 1% penicillin/streptomycin in a tissue culture incubator at 37.0 °C under 5% CO_2. All cell lines are tested for mycoplasma using e-Myco™ Mycoplasma PCR detection kit (Intron Biotechnology, Seongnam, Korea).

Crizotinib and SGX-523 were purchased from Selleck Chemicals (Houston, TX, USA), erlotinib from LC laboratories (Woburn, MA, USA), and lorlatinib (PF 06463922) from Toronto Research Chemicals (Toronto, Canada).

Drug sensitivity assays

Growth inhibition was measured using a modified 3-(4,5-dimethylthiazol-2-yl)-2,5-diphenyltetrazolium bromide (MTT) assay. Cells were plated onto 96-well plates at a density of 4,000 per well and continuously exposed to each drug for 96 h [2]. Analysis was performed running a nonlinear regression (curve fit) method in GraphPad Prism 7 for windows (GraphPad Software, San Diego, CA, USA).

Direct sequencing and mRNA expression analysis

RNA was extracted from cells using an RNeasy Mini Kit (Qiagen, Venlo, The Netherlands) according to the manufacturer's protocol. Direct sequencing was conducted as described previously [3]. RNA expression was analyzed by real time quantitative reverse transcription-PCR (qRT-PCR) of cDNA using TaKaRa SYBR Premix Ex Taq II (Tli RNase H Plus) (TaKaRa), according to the manufacturer's protocol. The primer information is provided in Supplementary Table S6.

Fluorescence *in situ* hybridization (FISH)

FISH was performed on formalin-fixed, paraffin-embedded samples by SRL Inc. (Tokyo, Japan) using a break-apart probe for the *ALK* gene (Vysis Break Apart Rearrangement Probe; Abbott Laboratories, Abbott Park, IL, USA), or *MET* SpectrumRed and *CEP7* SpectrumGreen probes, respectively. *ALK* fusion positive was defined as > 15% split signals in cells. *MET* gene amplification was defined as *MET*/*CEP7* ratio > 5.

Immunohistochemistry (IHC)

IHC was conducted as described previously [4]. Antibodies information is provided in Supplementary Table S7.

Western blotting and receptor tyrosine kinase assay

Western blotting was conducted as described previously [3, 5]. Antibodies information is provided in Supplementary Table S8. A Human Phospho-Receptor Tyrosine Kinase (RTK) Array Kit was purchased from R&D Systems (Minneapolis, MN, USA) and used according to the manufacturer's recommendations. Bands and dots were detected using an ImageQuant LAS-4000 imager (GE Healthcare Biosciences).

Xenograft models

Female BALB/c-nu/nu mice were purchased at 7 weeks of age from Charles River Laboratories, Yokohama, Japan. Cells (5×10^6) (ABC-14 or ABC-17) were injected subcutaneously into the backs of the mice. Treatment was started when the tumor reached approximately 250 mm^3 (day 0). Mice were randomized to receive vehicle, alectinib (10 mg/kg/day), crizotinib (50 mg/kg/day), erlotinib (25 mg/kg/day), or crizotinib + erlotinib for the same duration for ABC-14 xenograft model mice. ABC-17 xenograft model mice were randomized to receive vehicle, alectinib, crizotinib, or lorlatinib (10 mg/kg/day). The vehicle and drugs were administered once daily, five times per week by gavage. Tumor volume ($width^2 \times length/2$) was determined periodically. Statistical data were analyzed on day 28.

All experiments involving animals were performed under the auspices of the Institutional Animal Care and Research Advisory Committee at the Department of Animal Resources, Okayama University Advances Sciences Research. The experimental protocol was approved by the Animal Care and Use Committee, Okayama University, Okayama, Japan (OKU-2017084, 2017085).

Statistical analysis

All statistical analyses were conducted using STATA/SE ver. 14.0 (College Station, TX, USA). Inter-group differences were analyzed by the two-tailed paired Student's t-test (group = 2) and the ANOVA Bonferroni's Multiple Comparison Test (group $\geq$ 3). *P*-value of <0.05 was considered significant.

mRNA expression profiling and tumor mutation burden analysis by NGS

Frozen lung tissues and metastatic lesions were obtained at the time of autopsy, immediately frozen in liquid nitrogen, and stored until use. RNA was extracted from frozen tissues using an RNeasy Mini Kit (Qiagen) according to manufacturer protocol. cDNA libraries were prepared using the TruSeq RNA Access Library Prep Kit (Illumina, San Diego, CA, USA) and RNA sequencing was performed on a HiSeq Sequencing System. Sequencing data were mapped and analyzed to calculate TPM (Transcripts Per Kilobase Million) values using the CLC Genomics Workbench (CLC bio, Aarhus, Denmark). Fifty hallmark gene sets obtained from the Gene Set Enrichment Analysis molecular-signatures database (v.6.2; http://software.broadinstitute.org/gsea/msigdb/index.jsp) were used to extract genes representing well-defined biological states of processes. Hierarchical clustering was performed and displayed by using cluster 3.0 (http://bonsai.hgc.jp/~mdehoon/software/cluster/software.htm) and Java treeview (http://jtreeview.sourceforge.net/). Based on the similarity in gene-expression patterns of cancer-related genes, an unrooted phylogenetic tree was analyzed using the hclust and as.phylo functions and displayed using the plot function in the RStudio environment (https://www.rstudio.com/). Tumor mutation burden (TMB) was calculated using the selected 341 genes in MSK-IMPACT ver 1 according to a previous report [6]. Briefly, we extracted the number of mutations in the selected gens from the NGS data. TMB was calculated by dividing the number of mutations by the total genomic area where mutations were reported (0.98 Mb). The threshold of high TMB was defined as over 13.8 mutations/Mb. RNA-seq data are available in the NCBI Sequence Read Archive (SRA) repository (PRJNA545223).

Targeted deep sequencing of the ALK kinase domain using NGS

Frozen lung cancer tissues and metastatic lesions were obtained at the time of autopsy, immediately frozen in liquid nitrogen, and stored until use. Genomic DNA from freshly frozen tissue samples was extracted using a QIAmp DNA mini Kit (Qiagen) according to manufacturer instructions. Target enrichment was performed using 100 ng of input DNA using the HaloPlex^{HS} system (Agilent Technologies, Santa Clara, CA, USA), which is a high-sensitivity, amplicon-based targeted sequencing method. The library was prepared based on manufacturer instructions for ClearSeq Cancer HS, ILM, which was designed to identify somatic variants in 47 cancer-related genes targeting known COSMIC hotspots found to be associated with a various types of cancers. Sequencing was performed using the MiSeq version 3 600-cycle kit (Illumina, San Diego, CA, USA) according to manufacturer instructions for paired-end sequencing (2 × 300 cycles).

The generated sequences were processed in-house using Agilent SureCall software (Agilent Technologies), which is used exclusively with the HaloPlex^{HS} system. Amplicon-based targeted sequencing data are available in the NCBI SRA repository (PRJNA545223).

Quantification of amphiregulin (AREG) by ELISA

Cells (2×10^5) were cultured in RPMI-1640 medium with 10% FBS for 24 h, washed with PBS, and incubated for 48 h in 2 mL of the same medium. The culture medium was harvested and centrifuged, and the supernatant was stored at −80 °C until analysis. The level of AREG was determined using Quantikine ELISA kits (R&D Systems) in accordance with the manufacturer's protocols. All culture supernatants were tested twice. Color intensity was measured at 450 nm using a spectrophotometric plate reader (Bio-Rad Model 680). The concentration of AREG was determined in comparison to the standard curve.

Combination Index Analysis

The constant-ratio design for the combination assay is highly recommended as it allows the most efficient data analysis [7]. The multiple drug effect analysis developed by Chou and Talaly, based on the median-effect principle, was used to calculate the combined drug effect [8]. ABC-14 cells were seeded in triplicate in 96-well plates and were treated with alectinib and SGX-523 or crizotinib and erlotinib at the indicated concentrations for 96 hours. Cell viability was assessed using the MTT assay. The combination indices (CIs) were calculated using the CompuSyn software (Combosyn; Paramus, NJ, USA) as developed by Chou TC et al. in 2010 [9]. The plots generated by the CompuSyn software demonstrate the Y-axis CIs, where CI <1, =1, and >1 indicate synergism, additive effect, and antagonism, respectively. The X-axis represents the fractional activity, which reflects the fraction of cells inhibited by the treatments relative to the vehicle control.

Supplementary Figure S1.

Clinical course of brain metastases. (i) Brain metastases at initiation of alectinib treatment. There were two brain metastases: one on the temporal lobe and the other on the parietal lobe. (ii) Brain metastases 1.5 months after alectinib treatment. Both metastases shrank after treatment. After failure of alectinib treatment, the lesions did not progress according to contrast-enhanced computed tomography (not shown). (iii) Brain metastases after cisplatin/pemetrexed treatment (before ceritinib treatment). A new brain metastasis was observed on the frontal lobe. (iv) Brain metastases after ceritinib treatment. Contrast-enhanced MRI was not be performed due to the allergic side effects elicited by the contrast agent. Brain metastasis was not evident.

Supplementary Figure S2.

Characteristics of the clinical samples and established cell lines. **A,** Pathological findings and FISH analysis of *ALK* (red, ALK 3′-; green, ALK 5′-) of the primary right lung tumor biopsy specimen (scale bars: 50 μm). **B,** Microscopic images of established cell lines, ABC-14 and ABC-17 (scale bars: 100 μm). **C,** *EML4-ALK* fusion sequence of established cell lines (ABC-14, ABC-17) and autopsy samples (primary lung, bilateral kidney, PDX tumor) detected by Sanger sequencing. Primary lung; transbronchial biopsy sample from primary right lung tumors, Autopsy lung; autopsied sample from right lung tumor, meta; metastatic lesion

Supplementary Figure S3.

BIM deletion check by Sanger sequence PCR in ABC-14 and ABC-17 cell lines. **A,** Schematic image of the *BIM* deletion polymorphism and the Sanger sequencing PCR of the deleted portion of *BIM* in ABC-14 and ABC-17 cell lines. **B,** Electrophoresis image of *BIM* PCR products. PC-9 (*BIM* deletion negative control), ABC-14, and ABC-17 cell lines were all negative for the *BIM* deletion polymorphism.

Supplementary Figure S4.

RNA sequencing data analysis. **A,** Gene expression profile in transbronchial biopsy sample from primary right lung tumor, primary cardiac effusion, established cell lines (ABC-14, ABC-17), subcutaneous tumor of the PDX model mouse, and the autopsy samples by RNA-sequencing. TPM values were calculated with CLC Genomics Workbench (CLC Bio, Aarhus, Denmark). **B,** RNA sequencing data of ALK kinase domain in established cell lines (ABC-14, ABC-17) and PDX model tumor. The sequencing data are focused on the *G1202R* point mutation in all samples (pointed as arrow). **C,** RNA sequencing data of the ALK kinase domain in primary tissue samples, pericardial effusion and autopsy tissue samples. Sequencing data focused on the G1202R point mutation in all samples (arrows). **D,** Patterns of *ALK* mutations resulting in the G1202R substitution in clinical samples according to Sanger sequencing.
ALK, anaplastic lymphoma kinase; autopsy lung, autopsied sample from the right lung tumor; lt, left; meta, metastatic lesion; NGS, next-generation sequencing; primary lung, transbronchial biopsy sample from primary right lung tumors; rt, right; TPM, transcripts per kilobase million.

Supplementary Figure S5.

Resistance mechanism of ABC-14. **A,** IHC for MET of ABC-14 and ABC-17 cell lines (scale bars: 50 μm). **B,** Comparison of the expression of MET and EGFR protein between ABC-14 and ABC-17 cell lines by western blotting. **C,** Phospho-receptor tyrosine kinase assays for ABC-17 cells. **D,** combination index analysis of ABC-14 cells treated with alectinib in combination with SGX-523 (blue curve) and with crizotinib in combination with erlotinib (red curve) simultaneously for 96 hours at molar ratios of 1:2 (alectinib:SGX-523 and crizotinib:erlotinib). Synergistic effects in ABC-14 cells are shown.

Supplementary Figure S6.

Resistance mechanism of ABC-17. **A,** Evaluation of EMT of established cell lines, ABC-14 and ABC-17, by western blotting. PC-9 cell is positive control of E-cadherin, and 293T cell is a positive control of vimentin. **B,** Evaluation of EMT of established cell lines, ABC-14, ABC-17, liver metastasis, and PDX tumor, by immunohistochemistry. The upper columns are E-cadherin, and the bottom columns are vimentin (scale bars: 50 μm).

Supplementary Figure S7.

Gene expression profiles using RNA sequencing

A, Expression of DNA damage repair genes in the primary transbronchial biopsy sample, primary cardiac effusion, established cell lines (ABC-14, ABC-17), subcutaneous tumor of the PDX model mouse, and the primary and the metastatic lesion of the autopsy samples **B,** Heat map image of gene expression profiles in the primary transbronchial biopsy sample, primary

cardiac effusion, established cell lines (ABC-14, ABC-17), subcutaneous tumor of the PDX model mouse, and the primary and the metastatic lesion of the autopsy samples. The red color shows high gene expression and the blue color shows low gene expression in the heat map image. **C,** Phylogram image of gene-expression profile in the transbronchial biopsy sample, pericardial effusion, subcutaneous tumor of the PDX model mouse, and the autopsy samples by RNA sequencing. Autopsy lung, autopsied sample from right lung tumor; lt, left; Primary lung, transbronchial biopsy sample from primary right lung tumors; meta, metastatic lesion; rt, right; TPM, transcripts per kilobase million.

Supplementary Figure S8.

Targeted deep sequencing of the ALK kinase domain using HaloPlexHS

A, B, Targeted deep sequencing data of ALK kinase domain in alectinib resistant plural effusion and autopsy tissue samples. Autopsy lung, autopsied sample from right lung tumor; lt, left; meta, metastatic lesion; rt, right.

Supplementary Figure S9. Summary of the mechanisms of therapeutic resistance. **A,B,** Mechanisms of therapeutic resistance in the established cell lines (ABC-14, ABC-17, and PDX tumors). ABC-14 cells displayed *MET* gene amplification and increased AREG secretion. The ALK G1202R mutation was present in ABC-17 cells and PDX tumors. Combined therapy with crizotinib and erlotinib or lorlatinib treatment represent potential treatment strategies for overcoming therapeutic resistance. Alec, alectinib; Crizo, crizotinib.

Supplementary Table S1. Clinical response to alectinib therapy.

Target lesion (mm)	**Baseline**	**Best overall response (Day 44)**	**Progressive disease (Day 107)**
Primary lung	41.7	23.8	17.0
Liver metastasis	42.3	10.5	51.4
Left renal metastasis	41.2	17.7	15.9
Left adrenal metastasis	42.9	25.5	20.8
Right renal metastasis	48.5	22.0	25.3
Total (mm)	216.6	99.5 (−54.1%)	130.4 (+31.1%)
Non-target lesion			
Plural effusion		CR	CR
Brain		CR	CR #
Mediastinal lymph nodes		nonCR/nonPD	
New Lesion		No	No

Brain lesions were evaluated with enhanced computed tomography at the point.
CR, complete response; PD, progressive disease

Supplementary Table S2. Clinical response to cisplatin/pemetrexed therapy.

Target lesion (mm)	**Baseline**	**Best overall response (Day 45)**	**Progressive disease (Day 133)**
Primary lung	13.1	10.9	13.9
Liver meta#1	42.3	14.5	29.0
Liver meta#2	27.7	12.5	11.1
Left adrenal meta	21.8	18.2	21.3
Right renal meta	37.3	12.4	51.3
Total (mm)	142.2	68.5 (-51.9%)	126.6 (+84.8%)
Non target			
Brain			PD
Liver meta#3		nonCR/nonPD	PD
New lesion		No	No

CR, complete response; PD, progressive disease

Supplementary Table S3. Clinical course of ceritinib therapy.

Treatment day	Clinical course
Day 1	Ceritinib 750 mg/day
Day 15	Drug withdrawal due to Gr2 nephrotoxicity
Day 19	Restart with ceritinib 750 mg/day
Day 28	Drug withdrawal due to Gr2 nephrotoxicity
Day 31	Discontinuance due to Gr3 anorexia and disease progression

Gr, Grade

Supplementary Table S4. Mutations in genes used to calculate TMB in pretreated lung cancer.

Chromosome	Gene Name	Region	Type	Reference	Allele
1	SDHB	17024074	SNV	C	T
1	MUTYH	45333296	SNV	C	T
2	MSH2	47412436	SNV	T	C
2	MSH6	47799512	SNV	G	A
2	CASP8	201272669	SNV	A	G
2	BARD1	214730491	SNV	G	A
3	MLH1	37020350	SNV	C	T
5	APC	112842867	SNV	A	G
5	CSF1R	150054324	SNV	G	A
7	PMS2	5977709	SNV	T	C
7	PMS2	5982890	SNV	G	A
7	PMS2	5987189	SNV	C	T
7	MET	116731699	SNV	C	T
8	NBN	89958806	SNV	A	G
9	PTCH1	95449242	SNV	G	A
9	TGFBR1	99138080	SNV	G	A
9	TSC1	132903756	SNV	C	A
10	FGFR2	121488002	SNV	T	C
11	ATM	108257583	SNV	C	T
11	ATM	108267246	SNV	G	A
11	ATM	108279499	SNV	A	G
16	TSC2	2065526	SNV	C	T
16	TSC2	2065541	SNV	C	G
16	TSC2	2070559	SNV	C	T
16	TSC2	2079567	SNV	G	A
16	CDH1	68829727	SNV	C	T
16	CDH1	68833497	SNV	T	C
17	TP53	7675056	SNV	C	T
17	NF1	31226505	SNV	T	C
17	NF1	31233137	SNV	T	G
17	NF1	31261810	SNV	G	A
17	BRCA1	43071164	SNV	C	A
19	JAK3	17838329	SNV	C	A

Supplementary Table S5. Mutation pattern in pretreated lung cancer.

Transversion : Transition = 5 : 28 (%Transition = 84.8%)

Ref	Allele				
	A	T	G	C	Total
A	0	0	4	0	4
T	0	0	1	5	6
G	9	0	0	0	9
C	3	10	1	0	14
Total	12	10	6	5	33

Supplementary Table S6. Primer sequences

(A) EML4-ALK Direct sequencing analysis (mRNA)		
No.1	Forward	5'-CGGTCCGCTGAATGAAGT-3'
	Reverse	5'-GGTGGGAGTAGCATTCTTGC-3'
No.2	Forward	5'-CCCTCTTCACAACCTCTCCA-3'
	Reverse	5'-TCGTCCTGTTCAGAGCACAC-3'
No.3	Forward	5'-AGGTGTATGAAGGCCAGGTG-3'
	Reverse	5'-TCCACTGGTGACAAACTCCA-3'
No.4	Forward	5'-GGTCCTTTGGAGTGCTGCTA-3'
	Reverse	5'-TAAACCAGGAGCCGTACGTT-3'
No.5	Forward	5'-ACCTCTGCCTACCACCTCCT-3'
	Reverse	5'-GGGATCCCAAGGAAGAGAAG-3'
(B) BIM deletion direct sequencing analysis (DNA)		
Wild Type	Forward	5'-CCACCAATGGAAAAGGTTCA-3'
	Reverse	5'-CTGTCATTTCTCCCCACCAC-3'
Deletion	Forward	5'-CCACCAATGGAAAAGGTTCA-3'
	Reverse	5'-GGCACAGCCTCTATGGAGAA-3'

Supplementary Table S7. Antibodies for immunohistochemistry

Antibodies	Source	Identifier
ALK	Abcam	ab17127
MET	Cell Signaling Technology	8198
E-Cadherin	Cell Signaling Technology	3195
Vimentin	Cell Signaling Technology	5741

Supplementary Table S8. Antibodies for western blotting

Antibodies	Source	Identifier
Phospho-ALK (Tyr1604)	Cell Signaling Technology	3341
ALK	Invitrogen	51-3900
Phospho-STAT3 (Tyr705)	Cell Signaling Technology	9145
STAT3	Cell Signaling Technology	4904
Phospho-EGFR (Tyr1068)	Cell Signaling Technology	3777
EGFR	Cell Signaling Technology	2232
Phospho-MET (Tyr1234/1235)	Cell Signaling Technology	3077
MET	Cell Signaling Technology	8198
Phospho-p44/42 MAPK (Erk1/2) (Thr202/Tyr204)	Cell Signaling Technology	9101
p44/42 MAPK (Erk1/2)	Cell Signaling Technology	9102
Phospho-Akt (Ser473)	Cell Signaling Technology	9271
Akt	Cell Signaling Technology	9272
E-Cadherin	Cell Signaling Technology	3195
Vimentin	Cell Signaling Technology	5741
GAPDH	Cell Signaling Technology	2118

References

1. Isozaki H, Yasugi M, Takigawa N, et al. A new human lung adenocarcinoma cell line harboring the EML4-ALK fusion gene. *Jpn J Clin Oncol* 2014;44:963-968.
2. Mosmann T. Rapid colorimetric assay for cellular growth and survival: application to proliferation and cytotoxicity assays. *J Immunol Methods* 1983;65:55-63.
3. Ninomiya K, Ohashi K, Makimoto G, et al. MET or NRAS amplification is an acquired resistance mechanism to the third-generation EGFR inhibitor naquotinib. *Sci Rep* 2018;8:1955.
4. Kudo K, Ohashi K, Makimoto G, et al. Triplet therapy with afatinib, cetuximab, and bevacizumab induces deep remission in lung cancer cells harboring EGFR T790M in vivo. *Mol Oncol* 2017;11:670-681.
5. Kato Y, Ninomiya K, Ohashi K, et al. Combined effect of cabozantinib and gefitinib in crizotinib-resistant lung tumors harboring ROS1 fusions. *Cancer Sci* 2018;109:3149-3158.
6. Zehir A, Benayed R, Shah RH, et al. Mutational landscape of metastatic cancer revealed from prospective clinical sequencing of 10,000 patients. *Nat Med* 2017;23:703-713.
7. Chang TT, Chou TC. Rational approach to the clinical protocol design for drug combinations: a review. *Acta Paediatr Taiwan* 2000;41:294-302.
8. Chou TC, Talaly P. A simple generalized equation for the analysis of multiple inhibitions of Michaelis-Menten kinetic systems. *J Biol Chem* 1977;252:6438-6442.
9. Chou TC. Drug combination studies and their synergy quantification using the Chou-Talalay method. *Cancer Res* 2010;70:440-446.

Supplementary Figure S1

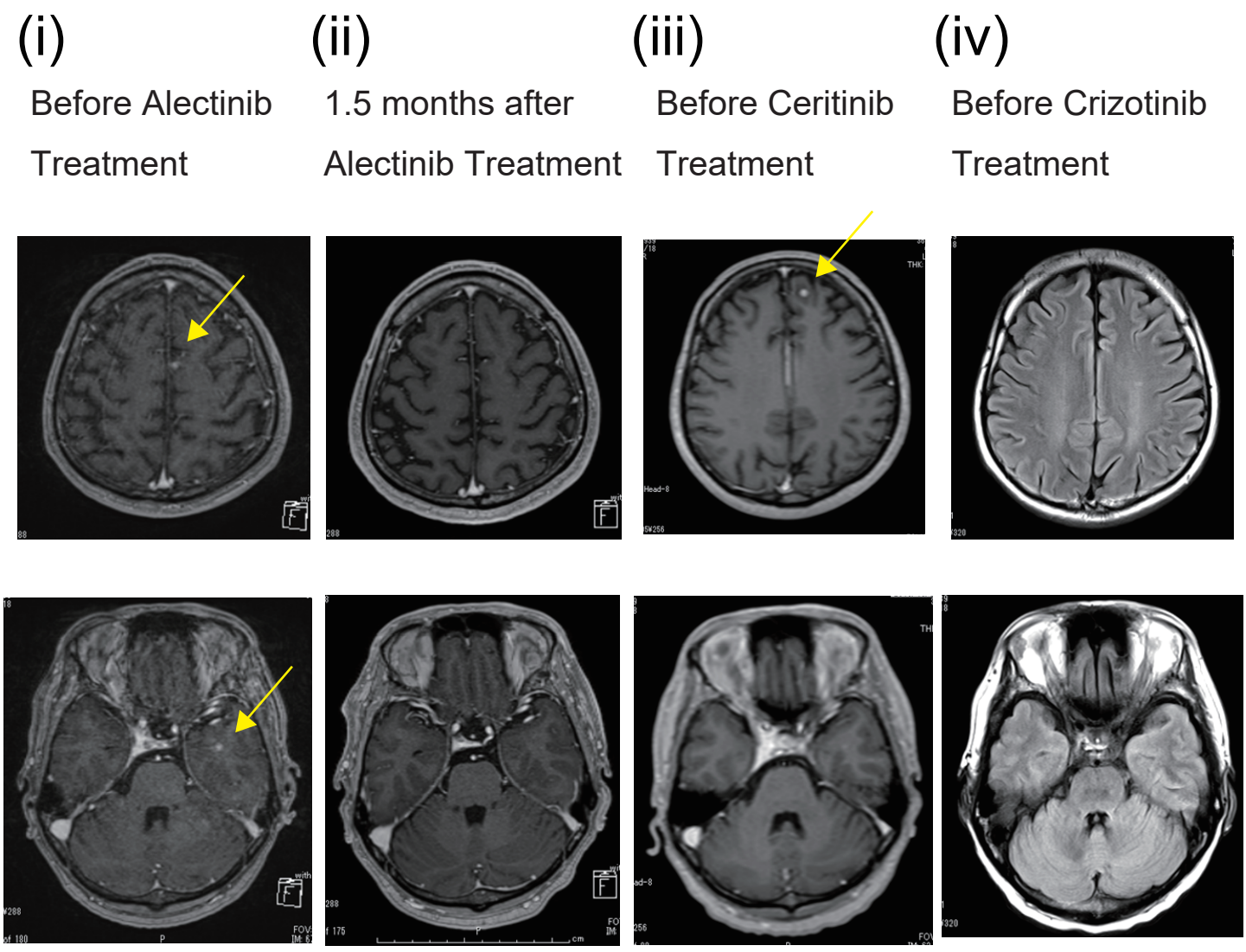

Supplementary Figure S2

A

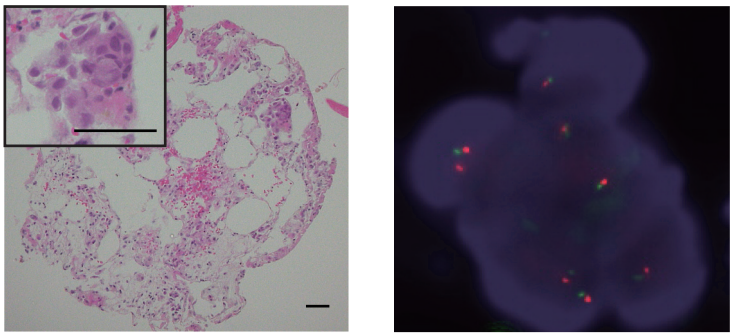

B

ABC-14

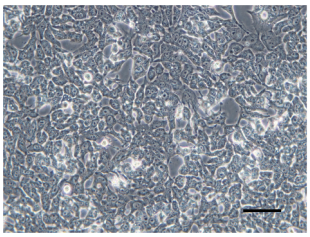

ABC-17

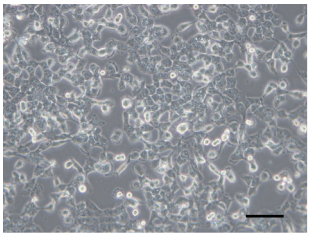

C

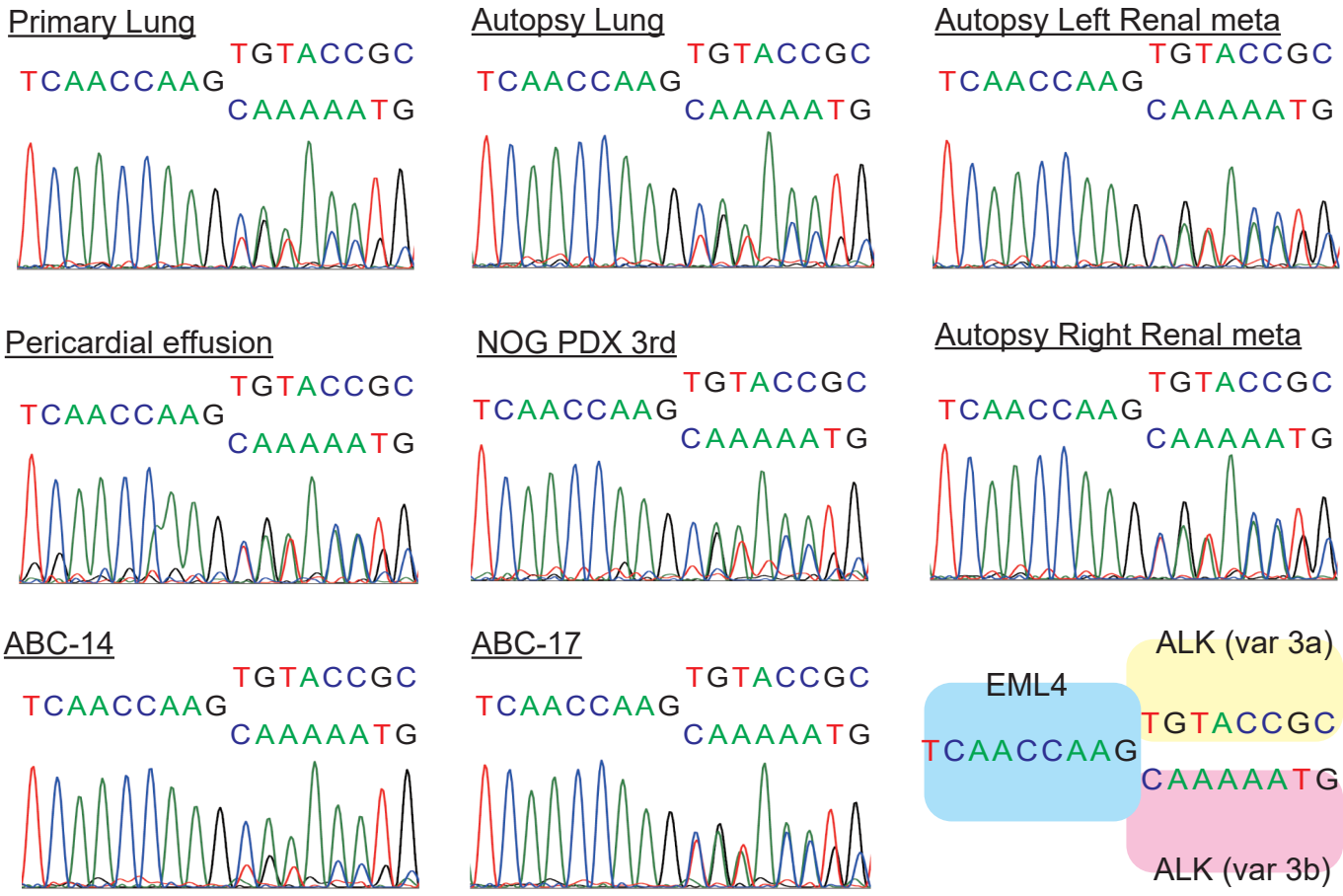

Supplementary Figure S3

A

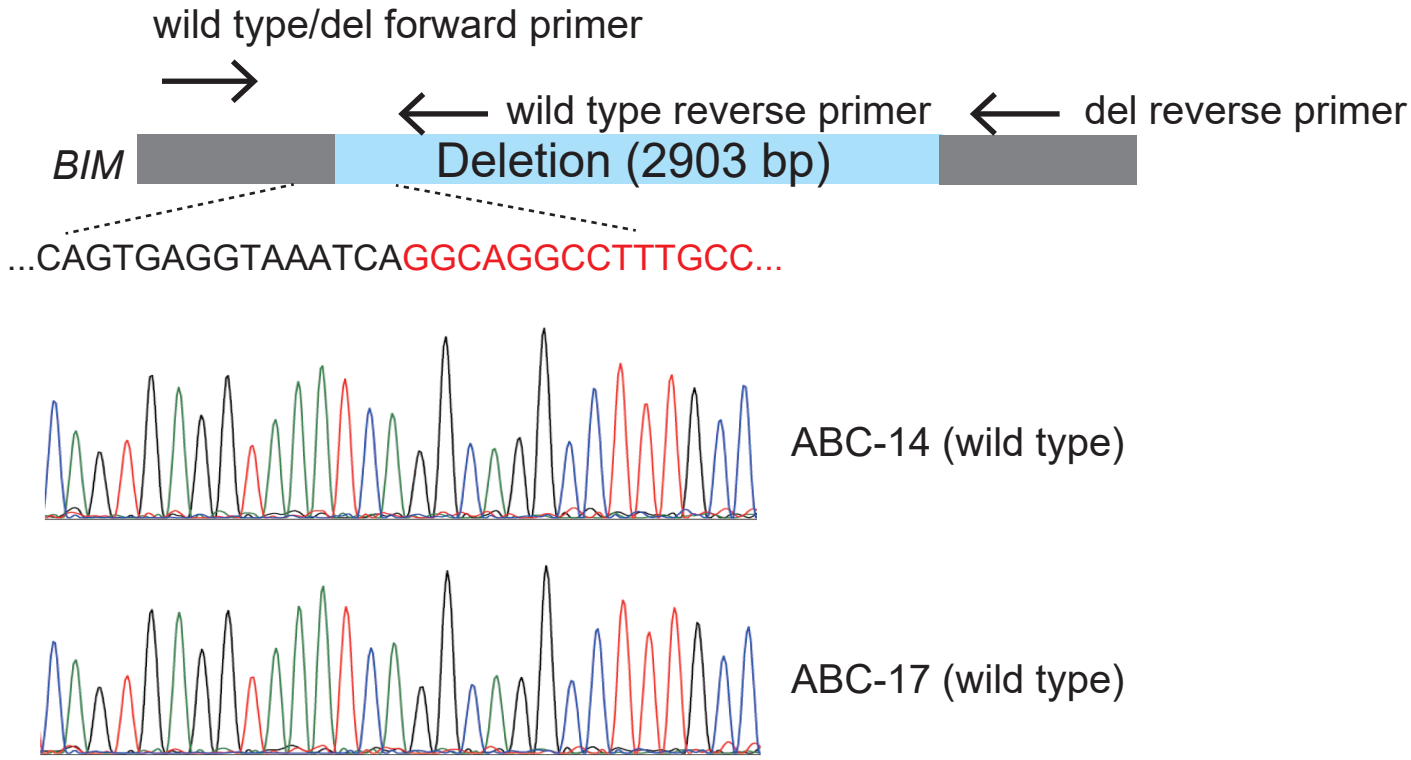

B

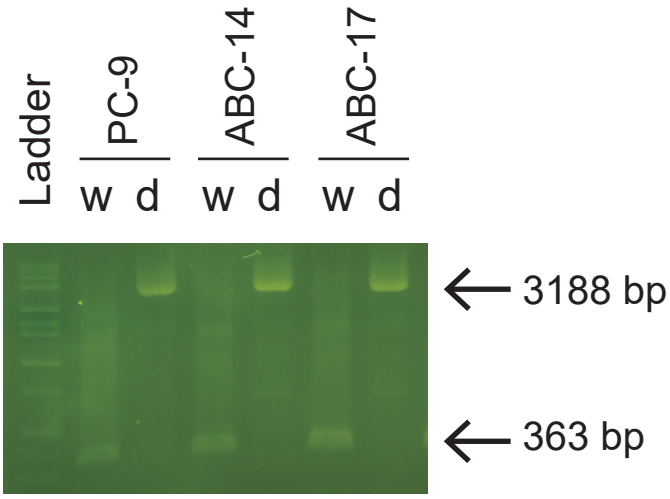

Supplementary Figure S4

A

Gene Name	ABC-14	ABC-17	Primary lung	Pericardial effusion	Autopsy lung	Autopsy liver meta	NOG PDX 3rd	Autopsy lt. renal meta	Autopsy rt. renal meta
EML4	29	22	41	29	37	7	2	27	14
ALK	14	19	5	2	5	6	1	1	6
MET	2,276	275	178	46	47	22	14	27	65
HGF	0	0	19	1	5	2	0	5	0
EGFR	124	66	59	11	53	34	4	23	47
EGF	14	9	4	1	5	6	1	5	4
TGFA	4	0	1	0	0	1	1	1	3
AREG	949	6	39	70	136	5	96	32	120
HBEGF	2	19	7	3	7	3	3	4	3
BTC	1	0	1	0	0	0	0	0	0
EREG	27	1	0	1	1	1	4	0	5
EPGN	0	0	0	0	0	2	0	0	0
VIM	48	2,638	1,684	552	1,119	126	29	512	456
CDH1	454	1	210	24	39	27	15	42	108

(TPM)

B

ABC-17:
C>T(G>A)

NOG PDX 3rd:
C>T(G>A)

ABC-14:
Wild Type

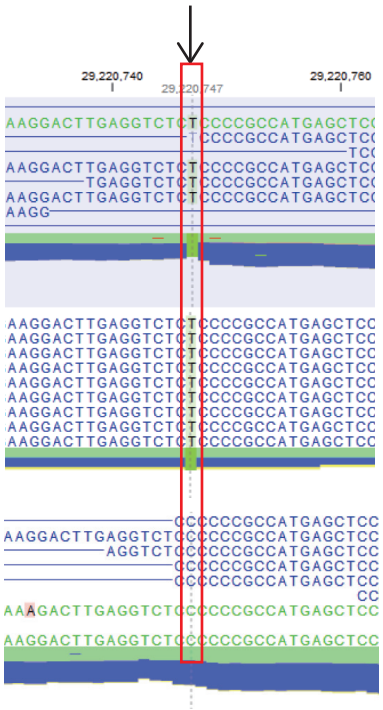

C

Primary lung:
Wild Type

Pericardial effusion:
Wild Type

Autopsy lung:
C>T(G>A)

Autopsy lt. renal meta:
Wild Type

Autopsy rt. renal meta:
C>G(G>C)

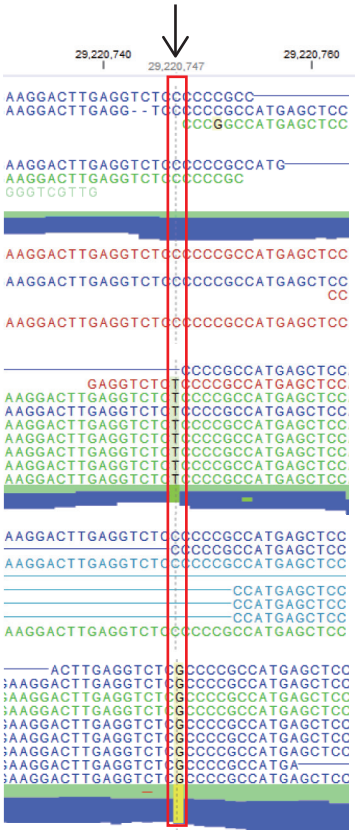

D

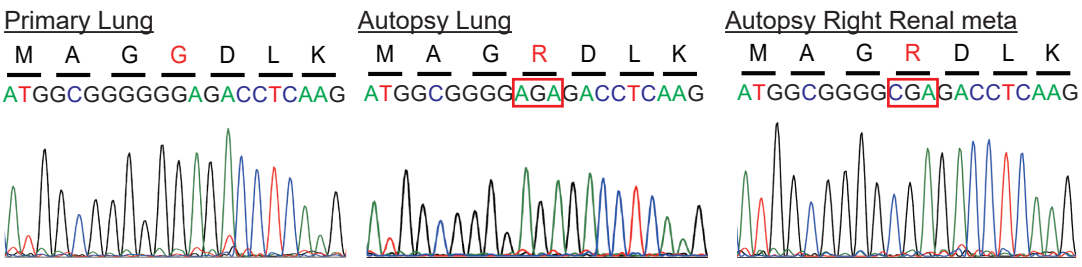

Supplementary Figure S5

A

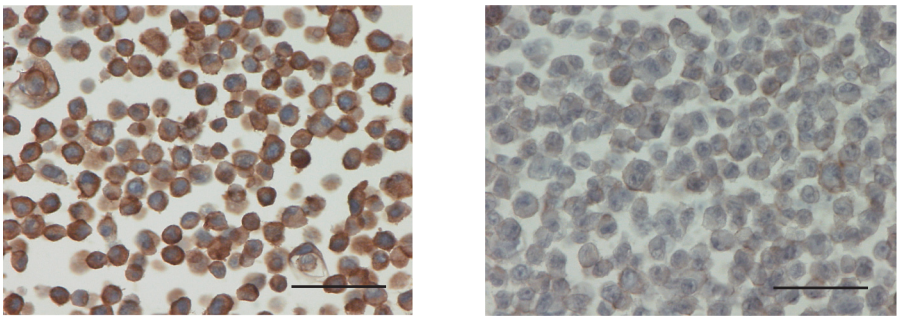

ABC-14 ABC-17

B

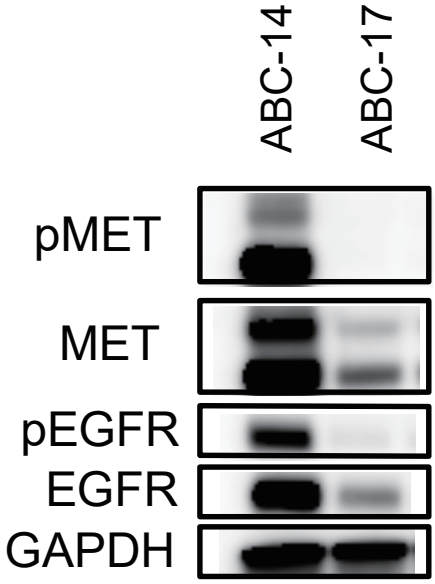

C

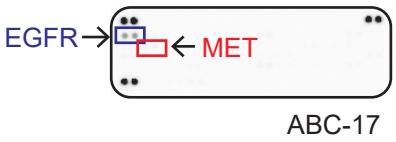

ABC-17

D

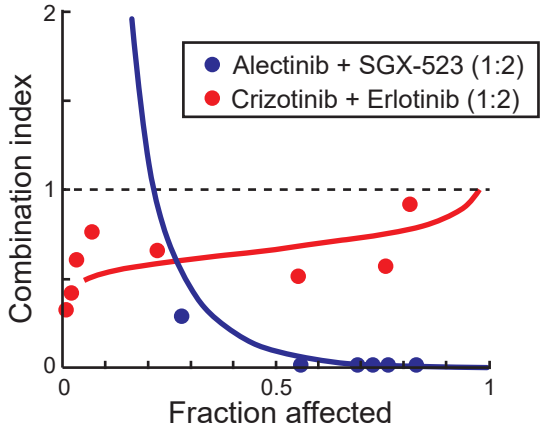

CI values at:

	ED50	ED75	ED90	ED95
Alectinib + SGX-523 (1:2)	0.101	0.015	0.003	0.002
Crizotinib + Erlotinib (1:2)	0.673	0.757	0.853	0.926

Supplementary Figure S6

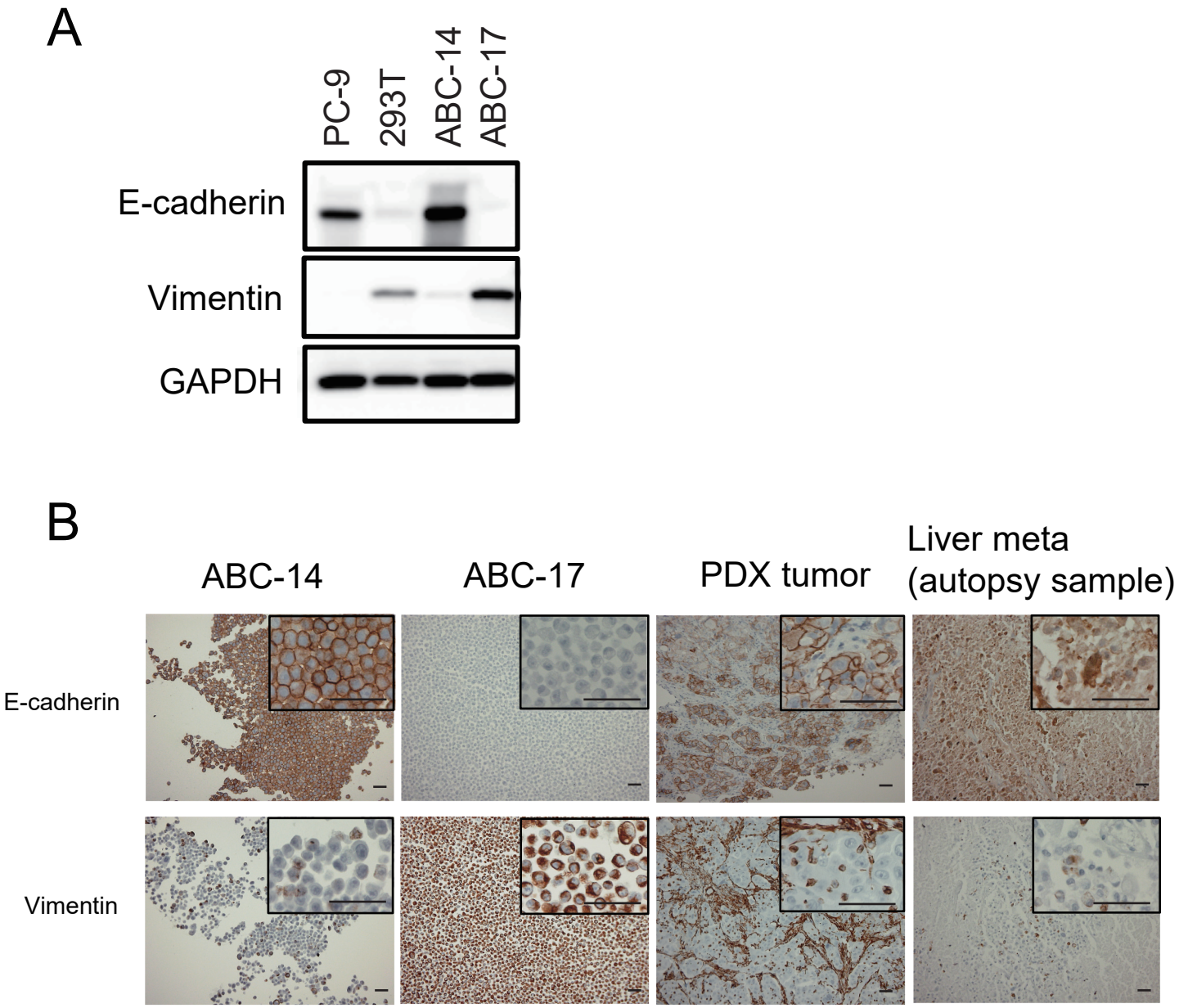

Supplementary Figure S7

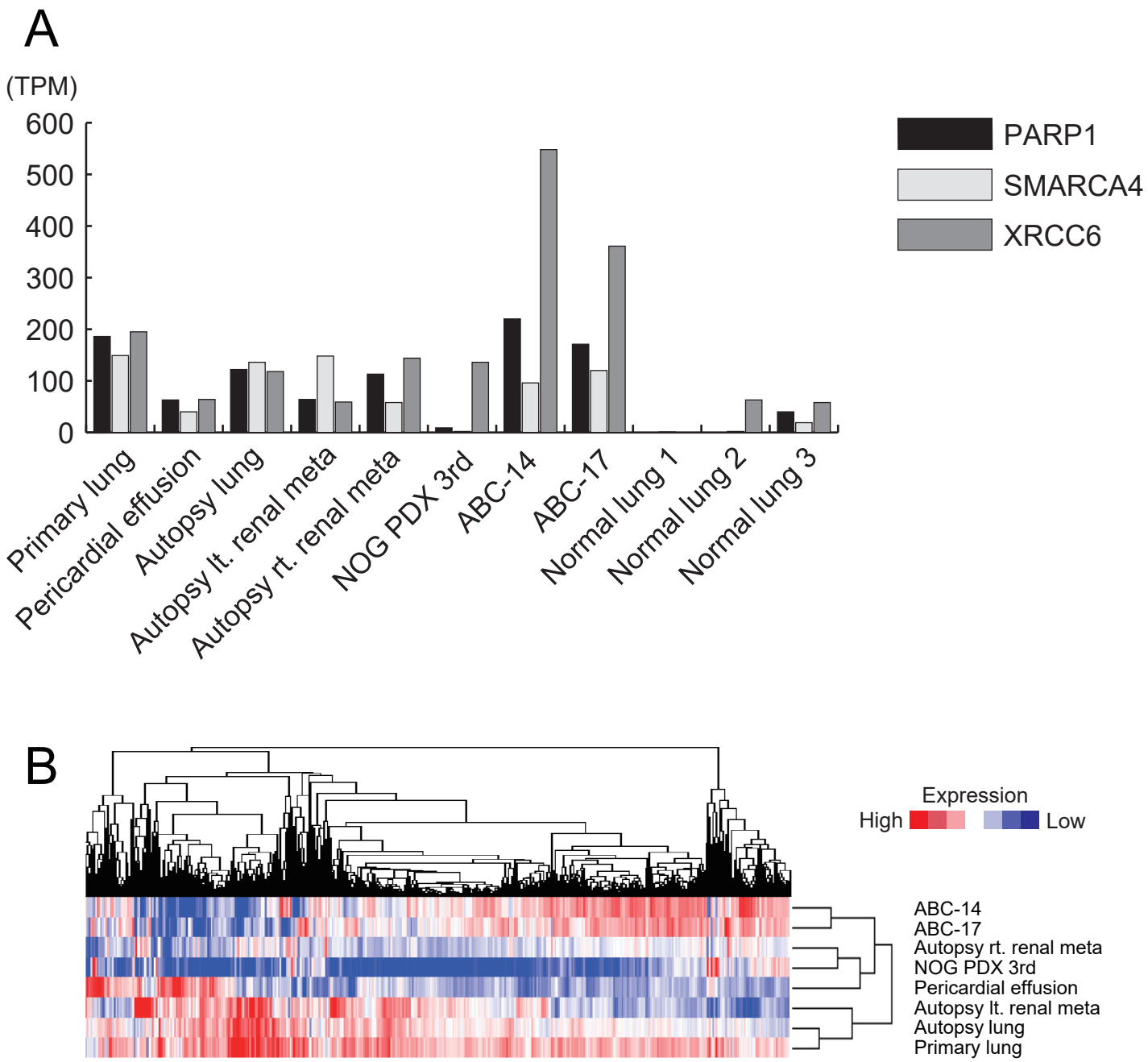

Supplementary Figure S8

A

ALK Gly1202Arg

	Codon 1202	Ref	Allele	Mutation count	Total read No.	% mutation
Alectinib resistant pleural effusion	GGA	G	G	0	28	-
Autopsy lung	**AGA**	G	A	2	55	3.64
Autopsy lt. renal meta	GGA	G	G	0	56	-
Autopsy rt. renal meta	**CGA**	G	C	6	88	6.82
Autopsy liver meta	**AGA**	G	A	12	51	23.5

B

Autopsy lung:
C>T(G>A)

Autopsy rt. renal meta:
C>G(G>C)

Autopsy liver meta:
C>T(G>A)

Supplementary Figure S9